

Factors Affecting the Optimal Sizing of
Generators and Storage in a Stand-Alone
Hybrid Renewable Energy System

Mohammad Shafiqur Rahman Tito

A thesis submitted to
Auckland University of Technology
in fulfillment of the requirements for the degree of
Doctor of Philosophy (PhD)

2015

School of Engineering

Abstract

There is a need to provide low cost electric power systems in a number of locations around the world. However, the size and cost of renewable energy generators and storage increase when they are used alone, due to the stochastic nature of sources. Reliability similar to the grid power supply can only be achieved by combining more complementary energy sources in the presence of storage devices; thus creating a hybrid renewable or distributed energy system.

The optimal sizing of a hybrid renewable energy system (HRES) is important in order to keep the system reliable with low investment cost and with adequate or full use of resources. In this work, the stochastic nature of renewable generation and demand and non-linear system characteristics are explored in the process of optimizing the size of a HRES. In achieving this, a hybrid optimization methodology was developed for the intention of matching the renewable generation with the demand of a site. The results showed that the demand profile dictates the size of a HRES and is as important as the optimization method.

In previous studies, average hourly demand profiles for a day, total monthly load, seasonal daily load profile, average hourly demand profile repeated throughout the year have been

examined, however, this work demonstrates that these demand profiles fail to represent real life electrical demand. As such, this work extends our understanding of the influence of demand, using multiple “real world” demand profiles, on sizing a HRES that result in varying temporal position of loads and the peak energy demand. It shows that the total daily demand of a site can vary significantly due to socio-demographic factors and that in sizing a HRES, the variation of the annual demand profile due to these factors must be considered.

Moreover, it furthers this by exploring the random day to day variations of peak demand both in magnitude and temporal position throughout the year that occur due to the varying weather conditions and habits of the user. It was determined that the effect of this random variation of electrical load on the optimal size of a HRES was significant and an advanced method for sizing a HRES under these conditions was developed and demonstrated.

Finally, a series of demand side management (DSM) options were proposed for the HRES and incorporated with the sizing method. It was shown that the investment costs could be significantly reduced with the introduction of each of the DSM options, in particular, by utilizing excess energy generated by the HRES to heat a thermal storage system.

Table of contents

List of figures	ix
List of tables	xiii
List of symbols and abbreviations	xv
1 Introduction	1
1.1 Importance of using renewable energy sources	1
1.2 Renewable energy sources	2
1.2.1 Geothermal energy	3
1.2.2 Solar energy	4
1.2.3 Wind energy	6
1.2.4 Hydro and micro-hydro	6
1.3 Stand-alone hybrid renewable energy system	7
1.4 Energy storage system	8
1.5 Sizing method for HRES	9
1.6 Electrical demand	13

1.7	Motivation	18
1.8	Scope of research	19
1.9	Contributions	20
2	System Model	23
2.1	Introduction	23
2.2	System configuration	24
2.3	Objective function formulation	24
2.4	Modeling of the system for optimization	27
2.4.1	Wind turbine generator model	30
2.4.2	Photovoltaic module model	32
2.4.3	Battery model	35
2.5	Reliability model based on loss of power supply probability (LPSP)	38
2.6	Optimization Methodology	39
2.6.1	Genetic algorithm	39
2.6.2	Exhaustive (iterative) search method	42
2.6.3	Hybrid (GA-exhaustive search) optimization method	44
2.7	Results and Discussion	46
2.7.1	Optimal size of a HRES for typical annual demand profile	46
2.8	Concluding remarks	49
3	Optimal Sizing of a HRES Considering Socio-Demographic factors	51
3.1	Introduction	51

3.2	Demand profile	53
3.3	Results and discussion	59
3.3.1	Optimal size considering socio-demographic factors	59
3.3.2	Reliability and system cost analysis	63
3.4	Concluding Remarks	67
4	Optimal Sizing of a HRES under Time Varying Load	69
4.1	Introduction	69
4.2	Demand profile	70
4.3	Sizing Methodology	71
4.3.1	Results and Discussion	73
4.4	Concluding remarks	77
5	Optimal Size Integrating Demand Side Management	79
5.1	Introduction	79
5.2	Demand profile	82
5.3	DSM Options	83
5.4	Optimization Methodology	84
5.5	Results and Discussion	84
5.5.1	Excess energy used for hot water and space heating	84
5.5.2	Peak demand reduced throughout the year	88
5.5.3	Peak demand reduced when SOC is low	90
5.5.4	Fraction of peak load shifted to off peak hours	93

5.6	Concluding remarks	95
6	Conclusion and Future Work	97
	References	101
	Appendix A	115
A.1	Investigation on Time Varying load	115

List of figures

1.1	Solar radiation that reaches the earth surface.	5
1.2	Hourly winter and summer load of typical house of a day	16
1.3	Classified six different profiles of a site based on socio-demographic factors	17
2.1	A Wind-Photovoltaic-Battery hybrid renewable energy system	25
2.2	Hourly wind speed (m/s) of a year in Auckland, New Zealand.	28
2.3	Hourly global horizontal radiation (W/m^2) of a year in Auckland, New Zealand.	28
2.4	Hourly temperature ($^{\circ}C$) of a typical year in Auckland, New Zealand. . . .	29
2.5	Average hourly electrical load profile of a day.	29
2.6	Power characteristic of a typical wind turbine generator (WG).	30
2.7	Flow chart of the implemented genetic algorithm (GA).	41
2.8	Flow chart of the implemented exhaustive search (iterative) method	43
2.9	Flow-chart of hybrid optimization method	45
3.1	Demand profile of Class #1 (high night use).	54
3.2	Demand profile of Class #2 (Similar morning and evening peak with low midday use).	55

3.3	Demand profile of Class #3 (high day use with morning peak).	56
3.4	Demand profile of Class #4 (extended evening peak).	57
3.5	Demand profile of Class #5 (medium flat day use with early evening peak).	58
3.6	Demand profile of Class #6 (low day use with evening peak).	59
3.7	Level and duration of the demand of a day.	64
3.8	Variation of battery SOC and generated renewable energy from 4000hrs to 5000hrs of a year.	65
3.9	Total system cost variation with the change of LPSP.	66
3.10	Variation of battery SOC for LPSP of 0.25 percent.	66
4.1	Hourly electrical load profile of a day.	71
4.2	Flow chart for generating approximate critical combination of annual demand profile.	74
5.1	Hourly winter and summer load of a day.	82
5.2	The variation of the SOC throughout the year for summer only demand.	86
5.3	The additional energy demand in winter session as compared to summer demand.	87
5.4	The excess energy generation from the system optimized only for summer load.	88
5.5	The modified winter load from 4140 hrs to 4280 hr of a year.	89
5.6	Electrical load is modified as per minimum SOC.	91
5.7	Modified load from hours 4140 to 4280 of a year.	92

5.8 The variation of the SOC throughout the year due to modified new load as
per minimum SOC 93

5.9 Modified demand shift as faction of winter load shifted from peak to off-peak
hours. 94

A.1 Hourly critical load of four days. 116

List of tables

2.1	Specification of the WG	32
2.2	Specification of the PV module	35
2.3	Specification of the battery	37
2.4	Approximate result with 300 Generation of a GA	46
2.5	Defining the bounds of decision variables using method I	47
2.6	The minimum and maximum values of the variables as found from the limited generation of GA	47
2.7	Defining the bounds of decision variables using method II	48
2.8	Optimal size of a HRES using hybrid method and GA for the average load profile of Fig. 2.5	49
3.1	Optimized size of a HRES for each of the profile classes	60
3.2	Pearson's correlation coefficient between average hourly solar radiation and wind speed with each of the demand classes	61
3.3	Cross LPSP results for each sized HRES	62
4.1	Optimal size of a HRES with typical annual demand	73

4.2	Optimal size of a HRES from three run of GA with random load variations .	75
4.3	Optimal size of a HRES for typical and critical hourly load profile	76
4.4	Probable optimal size of a HRES for hourly varied random load profile . . .	76
4.5	Probable optimal size of a HRES for hourly varied random load profile . . .	77
5.1	Optimal size of the system for summer only and seasonal variations	85
5.2	Optimal size of a system for summer for curtailed load due to seasonal variation	90
5.3	Optimal size of a system for modified demand as per minimum SOC	92
5.4	Optimal size of a system with reduced and shift of peak demand	95
A.1	Comparison of annual total load and LPSP	117

List of symbols and abbreviations

α	Power law coefficient
β	Photovoltaic tilt angle
β_{max}	Maximum tilt angle of a PV module
β_{min}	Minimum tilt angle of a PV module
δ	Declination
η_{bat}	Efficiency of a battery
ω	Solar hour angle
ϕ	Latitude of a site
ρ_g	Ground reflectance
σ	Self discharge rate of a battery
A_{WG}	Total swept area of a WG
C_n	Total capacity of batteries

C_{bat}	Capital cost of a battery
C_{bat}	Nominal capacity of a battery
C_h	Capital cost of a per unit height of WG tower
C_{PV}	Capital cost of a photovoltaic module
C_{WG}	Capital cost of a WG
D	Diffuse components of hourly global radiation
E_A	Available energy from a HRES
E_{avail}	Available energy from a system
E_{re}	Total amount of renewable energy
El	Energy demand of a site
$f(x)$	Objective function of variable x
$FF(t)$	Fill factor
$G(t, \beta)$	Global solar irradiance incident on a PV module at a tilt angle of β°
h	WG installation height
h_{max}	Maximum height of a WG tower
h_{min}	Minimum height of a WG tower
I_{SC-STC}	Short circuit current under STC

$I_{SC}(t, \beta)$	Short circuit current of a PV module
k_T	Sky clearness index
K_I	Short circuit current temperature coefficient
K_V	Open circuit voltage temperature coefficient
LP	Loss of power
M_{bat}	Annual maintenance cost of a battery
M_h	Annual maintenance cost of per unit height of a WG tower
M_{PV}	Annual maintenance cost of a PV module
M_{WG}	Annual maintenance cost of a WG
N_P	Number of photovoltaic modules connected in parallel
N_S	Number of photovoltaic modules connected in series
N_{bat_min}	Minimum number of battery
N_{bat_max}	Maximum number of battery
N_{bat}	Total number of batteries in a system
N_{Pbat}	Number of batteries connected in parallel
N_{PV_max}	Maximum number of PV
N_{PV_min}	Minimum number of PV

N_{PV}	Number of photovoltaic modules
N_{Sbat}	Number of batteries connected in series
N_{WG_max}	Maximum number of WG
N_{WG_min}	Minimum number of WG
$NCOT$	Nominal cell operating temperature
$P_{available}$	Power available from the system
P_{LOAD}	Demand
P_{PV}	Power produced by PV modules
P_{WG}	Power produced by WGs
P_w	Specific power output of a WG
T_A	Ambient temperature
v	Wind speed at hub height
V_{BUS}	DC bus voltage
v_{ci}	Cut-in speed of WG
v_{co}	Cut-out speed of WG
V_{OC-STC}	Open Circuit voltage under STC
$V_{OC}(t, \beta)$	Open circuit voltage

v_{ref}	Wind speed at referenced height
v_r	rated speed of WG
y_{bat}	Expected number of battery replacement during life of project
η_{PV}	Efficiency of PV modules and corresponding converters
η_{WG}	Efficiency of a WG and corresponding converters
CAES	Compressed air energy storage
DOD	Depth of Discharge
DP	Dynamic programming
DSM	Demand side management
EA	Evolutionary algorithm
GA	Genetic algorithm
GW	Giga watt
HRES	Hybrid renewable energy system
HSWSO	Hybrid solar wind system optimization
LP	Linear programming
LPS	Loss of power supply
LPSP	Loss of power supply probability

MCFC	Molten-carbonate fuel cells
MW	Mega watt
NMS	Nelder-Mead Simplex
PHS	Pumped hydrolic storage
PSO	Particle swarm optimization
PV	Photovoltaics
QP	Quadratic programming
RAPSODY	Remote area power supply optimization using dynamic programming
SA	Simulating Annealing
SMES	super Conducting Magnetic Storage
SOC	State of charge of batteries
STC	Standard test condition
TMY	Typical meteorological year
WG	Wind turbine generator

Declaration

I hereby declare that except where specific reference is made to the work of others, the contents of this dissertation are original and have not been submitted in whole or in part for consideration for any other degree or qualification in this, or any other university. This dissertation is my own work and contains nothing which is the outcome of work done in collaboration with others, except as specified in the text and acknowledgments.

.....

(Mohammad Shafiqur Rahman Tito)

November, 2015

Acknowledgements

I am grateful to Allah, the almighty for his guidance and infinite blessing for completing this difficult task successfully. This research work is supervised by Prof. Tek Tjing Lie and Dr. Timothy Anderson. I am highly grateful to both of them for their valuable and priceless guidance. Without their help and support, it would not be possible to complete this work. I would like to express my heartiest gratitude to both Prof. Tek Tjing Lie and Dr. Timothy Anderson for their keen interest and technical support throughout my study period.

I would like to express my deepest gratitude to my parents for their supportive and valiant role in every affair in my life. Special thanks and gratitude go to my lovely wife who sacrifices her career for the sake of my work, is always supportive and takes care during the anxious period of my work. I am also grateful to my loving son who has been deprived from my love and time during the period of my work.

I would also like to express my thanks to my colleagues for their technical and moral support.

Chapter 1

Introduction

1.1 Importance of using renewable energy sources

According to the World Bank, more than two billion people in the world live in remote villages that are not yet connected to utility lines [1, 2]. The extension of utility grids is not a feasible option for those villages due to the high investment cost. Diesel generators are costly as well as a source of pollution and so renewable sources are the only low cost and green option for those remote locations.

More broadly fossil fuels such as oil, gas and coal are exhausting rapidly. Though the statistics of fossil fuel reserve varies, it is estimated that world oil and gas reserves can only last for roughly 40 and 60 years respectively and coal is thought to be coming to an end in another 200 years [3]. Thus, it becomes necessary to look for a alternative energy sources to cater for the increasing demand of the world.

Global environmental concern is another key reason for moving to renewable energy. Carbon dioxide is naturally present in atmosphere and constantly being produced and absorbed by many microorganisms, plants and animals in the ocean and on the lands surface. The carbon cycle of emission and removal by natural processes tends to balance the carbon dioxide in the atmosphere. However, human activities such as the generation of electricity from fossil fuel, transportation and industrial processes dramatically increases the main greenhouse gas, carbon dioxide [4].

Technologies related to renewable energy sources such as solar and wind energy have developed to such an extent that the cost of the renewable energy has become comparable to energy from conventional sources. The average wholesale prices of conventional power varied approximated from 25 USD/MWh to around 100 USD/MWh in the year 2012 [5]. On the other hand, the cost of the onshore and offshore wind generation at utility scale reached 150 USD/MWh and 350 USD/MWh respectively, and solar PV at utility and small scale reached to 250 USD/MWh and 400 USD/MWh respectively [5].

1.2 Renewable energy sources

Renewable energy is abundantly available in different forms all over the world and most of them are cost free and sustainable. As a result, several renewable energy options have already become popular. They are:

1. geothermal,
2. wind,
3. solar and
4. hydro and micro-hydro.

They are briefly discussed below:

1.2.1 Geothermal energy

The thermal energy generated and stored inside the earth can be used directly for space heating and generating electricity. The internal structure and the physical process of the planet Earth are responsible for the inexhaustible quantities of thermal energy in the Earth's crust and is also cost effective, reliable and green [6]. The average geothermal gradient is around 30° C per km of depth [7]. With the temperature at the core-mantle boundary being over 4000° C.

A carrier, which is essentially rainwater, is used to extract the heat at accessible depths underneath the Earth's surface for utilization. The carrier is stored in a reservoir covered by impermeable rocks so that hot fluids can not easily reach to the surface and thus keep them under pressure. The fluid is extracted by drilling a well into the reservoir.

The installed electrical energy generation from geothermal resources reached 7974 MW in the year 2000 and the generated electrical energy represents 0.3% of total electrical energy

generation [7]. About 13% of the total electrical supply in New Zealand is sourced from geothermal energy [8]. Among other countries the Philippines, El Salvador, Nicaragua Costa Rica and Kenya produce significant amount of electricity from geothermal sources.

1.2.2 Solar energy

The sun is a source of abundant energy and approximately around 1.7×10^{17} W reaches to the earth and its atmosphere [9]. If only one percent of the received energy on the earth's surface could be converted into useful energy with an efficiency of 10%, solar energy could meet the total energy requirement of the world. Unfortunately most of the energy is lost in the atmosphere by scattering and absorption. Only a fraction of the extraterrestrial solar radiation reaches the surface of the earth with essentially no change in direction and it is called direct or beam radiation. The fraction of solar radiation that is scattered in the sky and comes back to earth is known as sky diffuse radiation. The direct solar radiation can be converted to useful energy with solar collectors. Fig. 1.1 [10] depicts the solar radiation that reaches the earth's surface after losses due to reflection, scattering and absorption as it passes through the atmosphere.

The amount of the direct solar radiation that reaches the earth surface depends on the cloudiness and position of the sun. The average annual direct normal solar radiation on the horizontal surface varies from 800 W/m^2 to higher than 1000 W/m^2 [11].

As solar energy is free from any pollution and its collection does not require any moving parts,

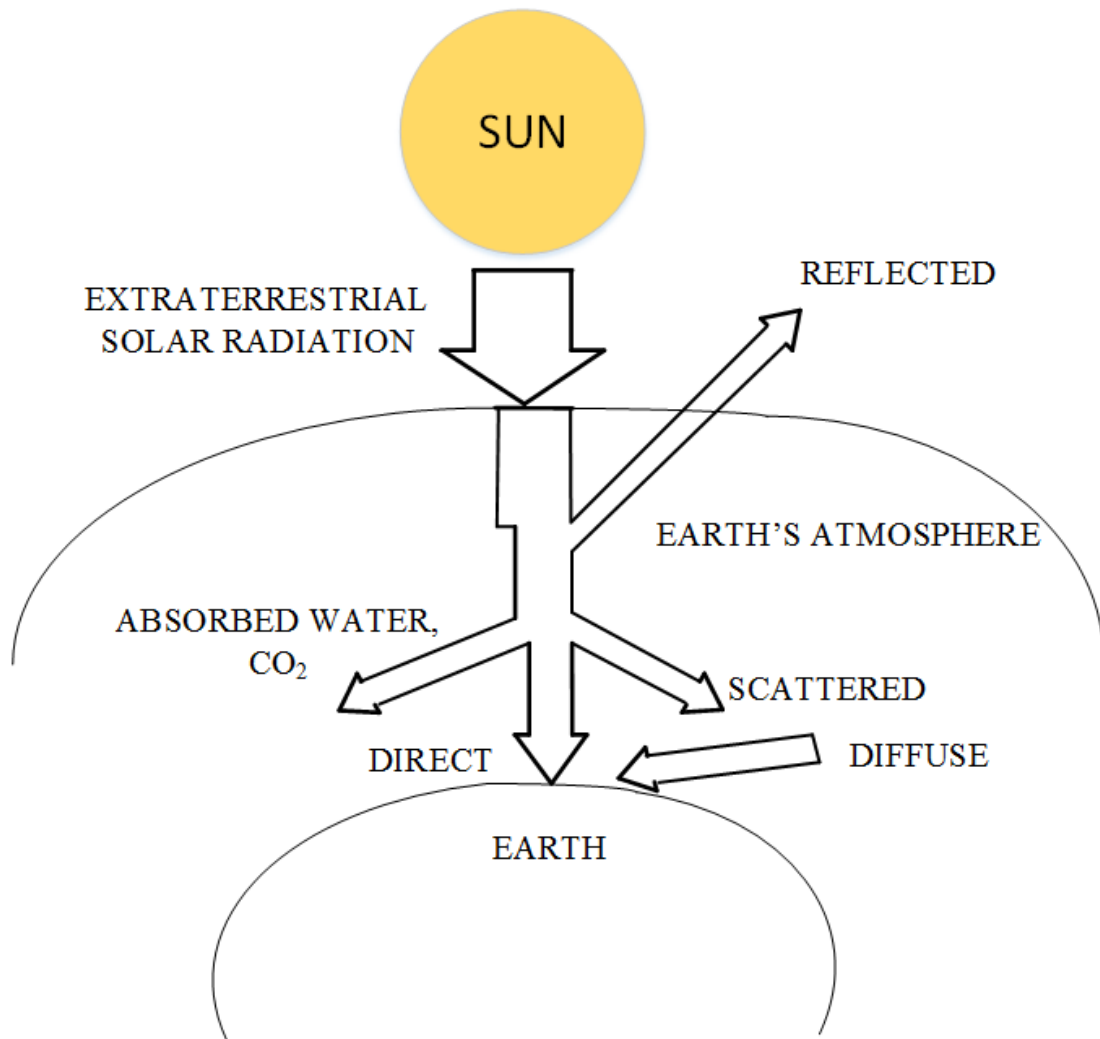


Fig. 1.1 Solar radiation that reaches the earth surface.

it does not require much maintenance. Moreover, with time solar energy technology has matured and its cost has reduced. As a result, the annual global installation of photovoltaics (PV) has expanded all over the world [12]. The total solar energy installation in worldwide has reached 135 GW in the year 2013 and continues to expand rapidly.

1.2.3 Wind energy

Wind energy is the oldest form of harnessed mechanized energy and is abundantly available in most parts of the world. It is low in cost, sustainable, safe, pollution free and is popular [3]. In contrast to the solar energy, it is potentially available 24 hours a day in a suitable site.

It is evident that sufficient wind is not only available on the land area but is also accessible in off-shore areas. However, offshore wind is under pressure due to the cost gap relative to more conventional (including onshore wind) energy sources. However, with the increased population of the world, the available land area has become scarce and off-shore wind farms are options for generating energy. It is also noticed that the cost of wind energy technology is decreasing day by day. With all these considerations, the on shore and off shore wind energy installations have increased dramatically in the last decade.

Global cumulative installed capacity of wind energy reached 318,105 MW in the year 2013 and the global annual installed capacity was around 35,289 MW in 2013 alone [13]. In New Zealand around 5% of total electricity is generated from wind energy and the target is set to 20% by the year 2030 [14].

1.2.4 Hydro and micro-hydro

Hydro power is one of the most important form of renewable energy used for generating electrical power. Hydro electric power comes from flowing water where the kinetic energy of flowing water is used to produce electricity. Both small and large scale implementation of

hydro-electrical power are possible. Small hydro often uses the flowing water of a river or dam. It provides approximately 19% of total global electrical energy generation [15] and about 57% of the total electricity generation in New Zealand [16].

Among these various options, wind and solar energy systems can be developed both in distributed (small scale) and centralized (utility scale) with cost comparable to existing grid power generated from fossil fuel. They can complement each other well in temporal distribution, thus, the storage requirement in matching the demand is reduced.

1.3 Stand-alone hybrid renewable energy system

As mentioned, renewable energy sources are only option for many remote locations in this world. The stochastic energy generation from renewable energy sources such as wind and solar may not match with the time distribution of demand [17] when they are used alone. Battery banks or hydrogen storage with electrolyzer and fuel cells or super capacitor are usually used as a backup power supply to satisfy the loads when energy from the renewable sources is not available. However, the problem associated with this kind of system is that the size of both the renewable generator and storage becomes extremely large. The solution to this problem is to integrate more than one complementary sources such as wind or photovoltaics in the presence of storage devices. Such a system is known as a hybrid renewable energy system (HRES) . The complementary power production capability of photovoltaics (PV) and wind turbine generators (WG) helps eliminate the weaknesses associated with each other

and reduces the requirement of energy sources as well as storage devices. A HRES which supplies energy in remote areas without any interconnection to external utility grid is known as a stand-alone HRES. Stand alone applications, PV and WG as a HRES promise to be a good alternative to grid extension or diesel generators if they are designed correctly [18]. Moreover, a WG-PV-battery system is considered as one of the most viable commercial configurations of HRES [19].

1.4 Energy storage system

The stochastic energy generation from renewable sources is often unable to meet a desired reliability criteria in the absence of any energy storage system. The application of any energy storage allows time shifting of generation by storing energy during off-peak hours and supply at peak hours. Energy storage technology can be classified as follows [20]:

- 1.** Electrical energy storage: (i) capacitors and super-capacitors store energy in electrostatic form and (ii) magnetic/current energy storage including super-conducting magnetic storage (SMES) .
- 2.** Mechanical energy storage: (i)kinetic energy storage (flywheels) and (ii) potential energy storage (pumped hydro storage and Compressed air energy storage (CAES)) .
- 3.** Chemical energy storage: (i) electrochemical energy storage (conventional batteries such as lead-acid, nickel metal hydride, lithium ion and flow cell batteries such as zinc bromine and vanadium redox) (ii) chemical energy storage (fuel cells, molten-carbonate

fuel cells (MCFC) and metal air batteries (ii) thermochemical energy storage (solar hydrogen, solar metal, solar ammonia dissociation – recombination and solar methane dissociation – recombination).

4. Thermal energy storage: (i) low temperature energy storage (ice slurries, cryogenic energy storage), (ii) high temperature energy storage (sensible heat systems such as steam or hot water accumulators, graphite, hot rocks and concrete, latent heat systems such as phase change materials).

1.5 Sizing method for HRES

An optimum mix and selection of each HRES device is crucial in order to make a system reliable and cost effective. The non-linear system characteristics, the random user demand and uncertain generation from WG and PV make the size optimization of a HRES more complicated. Therefore, an optimization method that matches the generation with the demand of a site, needs to be applied to ensure the lowest investment with adequate and full use of resources. A number of different optimization methods have been suggested for this purpose so far. The optimization methods can be classified as follows:

1. graphical construction methods,
2. exhaustive search (iterative) methods,
3. probabilistic methods,
4. heuristic methods and

5. hybrid methods.

A problem with one or two variables can be optimized using a simple graphical construction technique [21]. This method is not effective for WG-PV-battery HRES optimization as there are many variables involved. In order to get an idea of optimum value, this method might be effective.

A trade off curve of PV module and WG was utilized in [22] for a desired loss of power supply probability (LPSP) . In [23] a graphical construction technique was presented to optimize theoretical size (m^2) of solar module and wind turbine.

An iterative optimization method is very simple and easy to carry out and is implemented by linearly changing decision variables from a minimum to a maximum value or by employing linear programming [24]. An algorithm for sizing PV array only, in a Wind-PV-battery hybrid system was presented in [25]. The same authors later presented a methodology to optimize the size of battery along with the number of PV modules in order to meet a desired loss of power supply probability (LPSP) [22]. Their study in [26] distinguished the serial connection of components from the parallel connection and introduced more accurate mathematical model in order to improve the methodology proposed in [22]. Further [27] presented a simple iterative procedure based on energy balance to determine optimal size of WG, PV and battery in a standalone wind, PV and hybrid wind/PV system. An iterative method based on the trade off among reliability, minimum cost and use of diesel generator was presented to select an optimal combination and size of a HRES in [28]. An iterative method

for sizing a PV/wind/battery was presented in [29]. This method was well suited to high wind potential regions [30]. In order to generalize the method given in [29] for any region, the method in [30] is modified by considering both wind and PV as primary source. A novel iterative method for the hybrid solar-wind system optimization sizing model (HSWSO) , was presented in [31] for a WG-PV-battery hybrid system, and a hybrid PV-WG-battery power system for remote telecom station was optimized using an iterative algorithm by [32] taking into consideration LPSP.

The iterative algorithm discussed so far could only optimize three sizing parameters – the number or capacity of PV modules, wind generator and battery for a given load. It was unable to optimize the PV module slope angle and wind turbine installation height which are believed to be important parameters in the case of a system optimization.

An alternative is linear programming (LP) which is a deterministic method employing seasonal/annual average values of resources (wind speed or solar radiation) and load for the analysis purpose. In their study, [33] presented an optimization method using the dynamic programming model ‘RAPSODY’ that was used for sizing and operation of remote area power supply. Similarly, [34] utilized a linear programming technique to minimize the cost by optimizing the size of PV and WG for a reliable power supply.

Further, heuristic methods can solve an optimization problem on the basis of experience and judgment and usually result in a good solution within a short time. Though the best

result is not always guaranteed with a limited number of iterations, an approximate to optimum can be obtained. However, the solution of many optimization problems using classical mathematical techniques, like linear-programming (LP), Nelder-Mead simplex (NMS) dynamic programming (DP), Quadratic programming (QP) are unlikely to be solved within a reasonable time due to computational complexity. The user might not also satisfy with only one solution of a given problem as they may want to choose a solution from a set of solutions. In recent decades heuristic optimization approaches like genetic algorithm (GA) , particle swarm optimization (PSO) , evolutionary algorithm (EA) and simulating annealing (SA) have been applied for hybrid renewable energy optimization. All of them usually start with not only one solution but rather a group of solutions from the solution space of a given problem.

A genetic algorithm (GA) was introduced into the optimization of a HRES in [35] to select the type and number of WGs, number of PV modules and number of batteries to satisfy a constant load demand. The tilt angle of the PV was kept constant and the height of the WG was not considered [35]. Reference [36] utilized GA to optimize a WG-PV-battery hybrid system with a diesel generator as an auxiliary power source, while [18] utilized GA and proposed a methodology to suggest an optimum set from a list of commercially available system devices. Further [17] showed that the annualized cost of the system could be reduced further with a compromise in reliability index, LPSP. The developed methodology was used to optimize a system for telecommunication relay station at a desired LPSP of 2%. Finally [37] utilized GA in order to size the system devices of WG-PV-Battery with diesel generators

under variable load conditions.

Particle swarm optimization (PSO) is another heuristic global optimization technique that has been successfully applied to size a hybrid power system. In [38] hybrid WG, electrolyzer, hydrogen tank-fuel cell was optimized using PSO for two different system configurations, while [39] optimized a hydrogen-based stand-alone wind-PV generating system considering component outages. Similarly [40] sized a WG-PV-battery hybrid system employing PSO. Outage probability of system components was included in this analysis as was done in [39].

From these studies, it was found that GA reaches close to the best result within a short time uses less iterations but a complete convergence of the algorithm requires a large number of iterations. As a consequence, the computational time required to get the best result is very long. It has been suggested that utilizing a hybrid optimization method such as the combination of GA and simplex algorithm in [41] could address this problem.

1.6 Electrical demand

Electrical demand is an important input parameter in the sizing method and dictates the size of a HRES. However, the stochastic nature of the electrical energy usage patterns makes it difficult to model electrical demand profile of a site. The load profile is usually determined by the switching “on” or “off” of an individual electrical appliances, and it is influenced by

various environmental, dwelling and occupant characteristics [42]. The factors that influence the energy consumption of a house are identified as follows [43]:

- floor area of a house,
- number of residents,
- geographical location,
- occupancy patterns,
- seasonal and daily factors,
- appliances level of ownership,
- fuel used for domestics hot water, space heating and cooking,
- social status,

These various factors can be grouped broadly in two categories. They are:- (i) socio-demographic factors and (ii) seasonal factors. The floor area and geographical location evidently belong to seasonal factors [43] whereas the remaining factors belong to socio-demographic factors. It was also shown in [44] that domestic energy consumption is influenced by the age of residents. The operation of some appliances such as television, video recorder, computer or laptops and others are linked with life-style-related psychological factor. The usage pattern of appliances is determined by single or multiple factors and shapes the load profiles.

The continuous and standby power use of cold and active appliances were investigated

for finding the period and duration of “switching on” in [45]. The continuous and standby power use of appliances found to be “on” over a 24 hours period form the base load of the profile along with the cold appliances. This energy consumption was classified as predictable and moderately predictable in [46]. The predictable energy consumption is independent of the user actions where as moderately predictable consumption is related to the habitual behavior of the occupant and is cyclical in nature. However, the consumed energy by the active appliances such as kettles and electrically heated showers are more random in nature and typically consume high power. The vast majority of electric appliances are in the group of active appliances and the energy consumption of these appliances in a house is unpredictable.

Further the external and internal temperature of a house is linked with seasonal variations and switching on and off of many appliances depends on the seasonal variations. Fig. 1.2 shows electrical load variations in summer and winter due to temperature variation in New Zealand.

An electrical load profile can therefore be considered as the combination of deterministic and stochastic process [42]. The electrical demand at any time can be assumed to be a combination of four separate components: the normal part, the weather sensitive part, the special event part and a random part [47]. The modeling of the deterministic part of electric load is easy, however, the stochastic nature of the random load is difficult to predict and is linked with many factors as discussed above. The base electrical load remains relatively constant throughout the year but the operation of many appliances is cyclic in nature and the

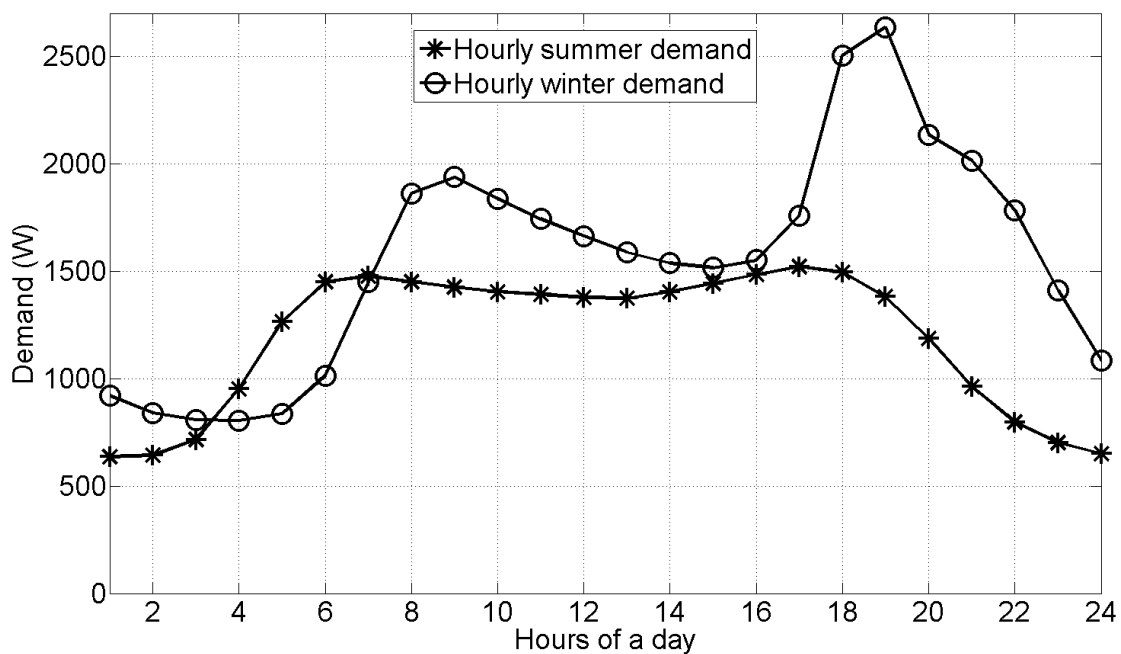


Fig. 1.2 Hourly winter and summer load of typical house of a day .

operating period of these cyclic appliances is not always fixed. As such the magnitude and temporal position of the stochastic portion of electric demand varies significantly.

The demand profile generator [48], a simulation tool was developed based on the studies of [44] to explore the effect of the usage patterns of different appliances on demand profiles. The data and information from [44, 49, 50] were used in developing that tool. They classified the appliances into different categories and probable operating time for each of these groups was identified. Each hour of the likely operating time was identified with a given probability. The washing machine as an example was classified in wet appliances category and set the operating period from 18:00 hr to 24:00 hr. Each hour has a probability of 0.2 except the hours 22:00 hr-23:00 hr and 23:00 hr-24:00 hr. The probability of operating a washing

machine at these hours was set to 0.1. This was also varied with number, age and status of the occupants.

As a result, the magnitude and temporal position of peak electrical demand varies day to day. Fig. 1.3 shows random variation of peak electrical demand for different types of users.

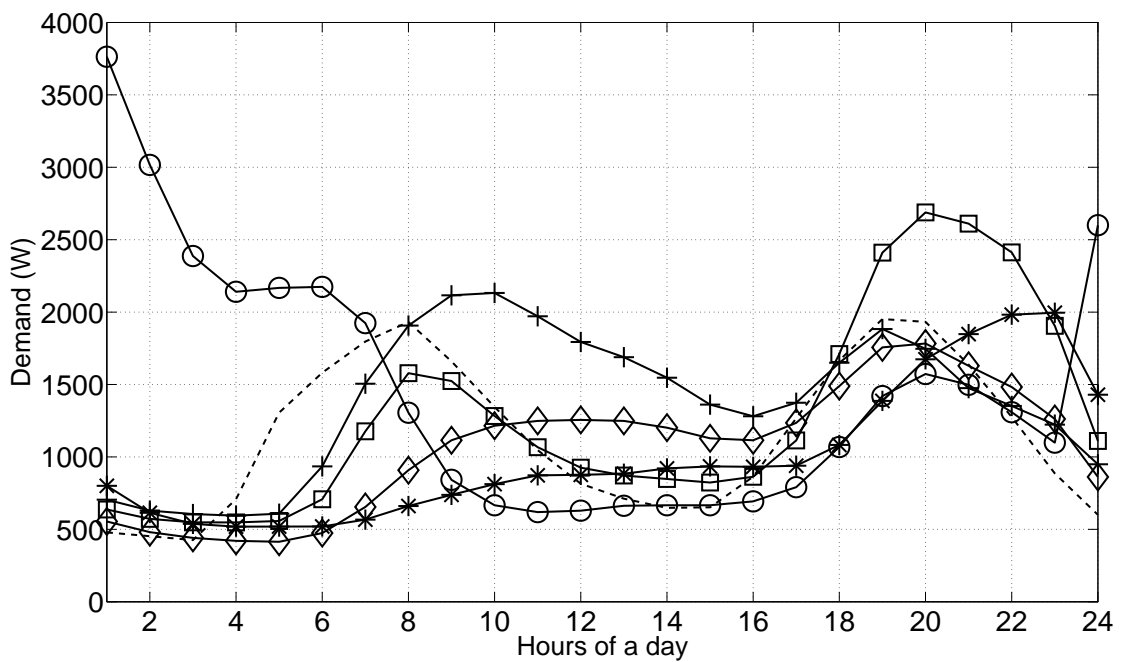


Fig. 1.3 Classified six different profiles of a site based on socio-demographic factors

Chronological modeling of electrical load keeping all these factors in mind is quite difficult and cumbersome. However, input of real life electrical load is as important as the sizing method.

1.7 Motivation

The optimal sizing methods usually match the variable generation from renewable sources with an existing demand of a site. It is therefore important to input a realistic demand profile to the method so that the optimized size would be able to meet with the desired reliability. Hourly electrical load of a day was considered in [25, 27] in sizing a PV module and a given wind turbine generator. Hourly generation and demand for a typical day in each month was taken into consideration for sizing PV modules and batteries in [22]. The average monthly demand data was considered in sizing the WG swept area and surface area of PV modules in [23, 51], while an hourly constant load was assumed in [17, 31, 52, 53]. The electrical load of an energy saving light and a street lamp which was turned on at night only was satisfied by PV modules and batteries for a fixed WG generation in [26] and [41]. Hourly demand for a day repeated throughout the year was examined for sizing a HRES by [18, 28, 29, 54, 55] and day to day demand variation of 30 percent was introduced with the hourly demand of a day in considering randomness of the load [37]. The load data for the IEEE reliability test system (IEEE RTS) [56] was taken into consideration in [39] and five different load profiles (constant low load, hourly domestic load, farm load, high load and continuous high load) were considered in [57]. Two days in a week, weekend and weekday load were taken into consideration in [58] in order to include the effect of the working pattern of the residents while sizing a HRES. Six different demand profiles were considered in [59] while using Fuzzy logic for sizing a HRES. The demand profiles included midday and midnight peak of summer and winter load as well as constant summer and winter demand, in order to consider the same

and varying annual electrical load. However, there is a greater need to include realistic load profiles in the sizing and optimization of HRES.

1.8 Scope of research

Optimal sizing of a HRES plays important role to ensure lowest investment cost as well as full use of system resources. The optimization method thus matches the generated energy from a HRES with a given demand in such a way that some constraints are satisfied. The demand which is the key driving input in sizing a power generating system [60], has not been given much attention so far for sizing optimization.

In most of the previous studies, the emphasis was given to the optimization method rather than the load profile of the site. In almost all the previous studies, the hourly demand of a day [17, 18, 25] repeated throughout the year or monthly average daily demand [22] or seasonal demand [23] was only considered during the sizing optimization of a HRES and so does not represent the real load of the site. The demand is usually stochastic in nature and varies both in magnitude and temporal position. The variation of the load depends on both internal and external factors [61]. The internal factors include the number and age of the house hold occupants, their social status, characteristics of building material and the external factor includes external temperature. The optimized size of HRES without considering this load variation fails to meet the desired reliability. Thus, the demand profile needs to be modeled considering the above mentioned factors while sizing a HRES.

1.9 Contributions

The research undertaken in this thesis has made the following contributions to advance the current state of the field.

- For many applications, particularly residential dwellings, this load is generally stochastic in nature and governed by a wide range of internal and external factors such as the socio-demographic characteristics of the households' occupants (like number and age of occupants, their working pattern and their social status) and also seasonal variations [61]. In this study, the socio-demographic factors are integrated while sizing a HRES.
- The hourly demand of a day repeated throughout the year does not represent real life load of a site. The load usually varies randomly both in magnitude and temporal position. This time varying demand variations is incorporated in optimal sizing of a HRES.
- DSM has attracted the attention of the system planners for its ability to modify the demand profile and thus can reduce the investment cost. The DSM program includes the use of efficient utilities, cutting off the peak demand, shifting the peak demand to the off-peak time etc. DSM can play a great role in optimal sizing of a HRES which has never been considered in any of the previous studies.

The following list of publications has been published as part of this research work.

1. Tito, MS Rahman, Tek T. Lie, and Timothy Anderson, "Sizing Optimization of Wind Photovoltaic Hybrid Energy System under Transient Load." *International Journal of Power and Energy Systems* 33.4 pp.168-174 (2013).
2. Tito, Rahman, Tek Tjing Lie, and Timothy Anderson, "A simple sizing optimization method for wind photovoltaic battery hybrid renewable energy systems." *ENZCON'13 Proceedings of the 20th Electronics New Zealand Conference*, Auckland, September 2013.

Chapter 2

System Model

2.1 Introduction

The optimal sizing of a HRES requires the power generation to be matched with the demand of a site. The estimation of power generation depends on the available resources at a site as well as the performance of the generators. A system simulation can provide a good estimation of power generation when it is correctly modeled. Quite often it is found that one renewable source is not able to provide sufficient power to meet the demand and so it is necessary to combine several complementary renewable sources and storage elements in a stand-alone application. The complementary nature of renewable sources reduces the size of the storage elements in a combination, thus delivering a low cost system.

2.2 System configuration

Numerous hybrid renewable energy systems have been investigated previously for stand-alone applications including wind-PV-battery, wind-PV-diesel generator, wind-PV-battery-diesel generator, PV-hydrogen storage-fuel cell and wind-PV-hydrogen storage-fuel cell [19]. However extensive research has developed PV and WG technologies to such an extent that they can compete as an economical alternative to conventional power generating systems. Therefore, among the available potential configurations of HRES wind-PV has proven to be commercially more viable than other options [19]. Similarly, for storage devices, batteries are one of the most common choices due to their low cost and advancement in technology. Thus, in this work, a wind-PV-battery hybrid renewable energy system is considered for further investigation as shown in Fig.2.1. For this system, the WGs, PV modules and batteries are considered to be connected to DC and AC loads through a 24V DC bus.

2.3 Objective function formulation

Sizing a hybrid renewable energy system correctly, requires a careful balancing and optimization of the generation and storage with respect to the demand for electricity placed on the system by the users. Therefore, it can be viewed as an optimization problem with a constrained variable that can be stated by equation (2.1)

$$\textit{maximize/minimize } f(x) \tag{2.1}$$

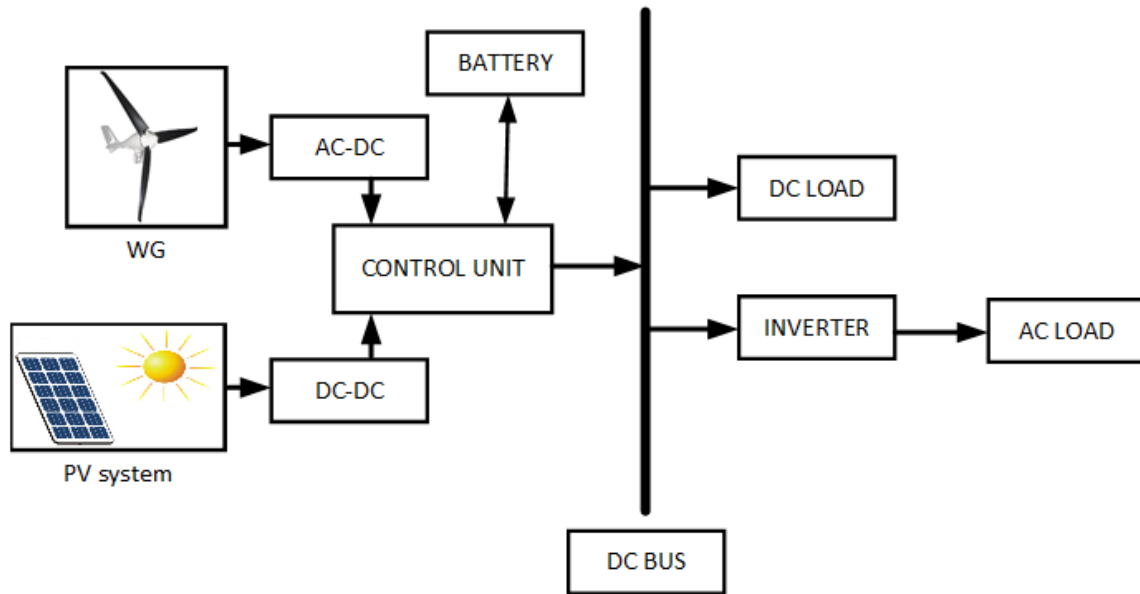


Fig. 2.1 A Wind-Photovoltaic-Battery hybrid renewable energy system

subject to the constraint in equation (2.2)

$$x_{min} \leq x \leq x_{max} \quad (2.2)$$

where $f(x)$ is an objective function.

For this study, the aim is to minimize the total cost of ownership over the life of a HRES while also maintaining an LPSP of zero. The total cost consists of the capital cost of WGs, PV modules and batteries and 20 years total maintenance in addition to the operational cost

of WGs, PV modules and batteries as given by equation (2.3) [18].

$$\begin{aligned}
 & \text{Minimize } f(N_{PV}, N_{WG}, N_{bat}, h, \beta) & (2.3) \\
 & = N_{PV}(C_{PV} + 20M_{PV}) \\
 & + N_{WG}(C_{WG} + 20M_{WG} + hC_h + 20hM_h) \\
 & + N_{bat}(C_{bat} + y_{bat}C_{bat} + (20 - y_{bat} - 1)M_{bat})]
 \end{aligned}$$

Subject to the constraints in equation (2.4):

$$\begin{aligned}
 N_{PV} & \geq 0, & (2.4) \\
 N_{WG} & \geq 0, \\
 N_{bat} & \geq 0, \\
 \beta_{max} & \geq \beta \geq \beta_{min}, \\
 h_{max} & \geq h \geq h_{min}, \\
 & \text{PV modules are assumed to be faced true North.}
 \end{aligned}$$

where, $N_{PV} = (N_S \times N_P)$ is the number of photovoltaic modules, N_{WG} is the number of wind turbine generators, $N_{bat} = (N_{Sbat} \times N_{Pbat})$ is the number of batteries, N_{Sbat} is the number of series connected batteries determined by the bus voltage, N_{Pbat} is the number of parallel connected batteries which is determined by the optimization, β is the photovoltaic tilt angle, h is the WG installation height, C_{PV} is the capital cost of a photovoltaic module, C_{WG} is the capital cost of a WG, C_h is the capital cost per unit height of a WG tower, C_{bat} is

the capital cost of a battery, M_{PV} is the yearly maintenance cost of a PV module, M_{WG} is the yearly maintenance cost of a WG, M_h is the yearly maintenance cost per unit height of a WG tower, M_{bat} is the yearly maintenance cost of a battery and y_{bat} is the expected number of battery replacements during a 20 year period.

2.4 Modeling of the system for optimization

In order to optimize the system, it is necessary to understand the environmental conditions in which the system will operate, as well as the demand that will be placed on the system. For this study it was assumed that the system would be installed for a single dwelling in Auckland, New Zealand (latitude 36.85° S and longitude 174.78° E). Figs. 2.2, 2.3 and 2.4 show hourly wind speed (m/s), solar radiation (W/m^2) and ambient temperature ($^\circ C$) across a typical meteorological year (TMY) data for Auckland that were used in the determination of the electrical output from the HRES [62].

In addition to understanding the prevailing weather conditions, that determine the output from the generators, it is also necessary to understand the typical loading conditions for the HRES. In [61], 239 electrical demand profiles from 40 houses were recorded and classified into six different classes based on the time of energy usage patterns. The average of these six classes as presented in Fig 2.5 was taken for this study. Close examination of the demand profile reveals that the electrical load is typically low (<1 kW) from 02:00 hr to 03:00 hr and

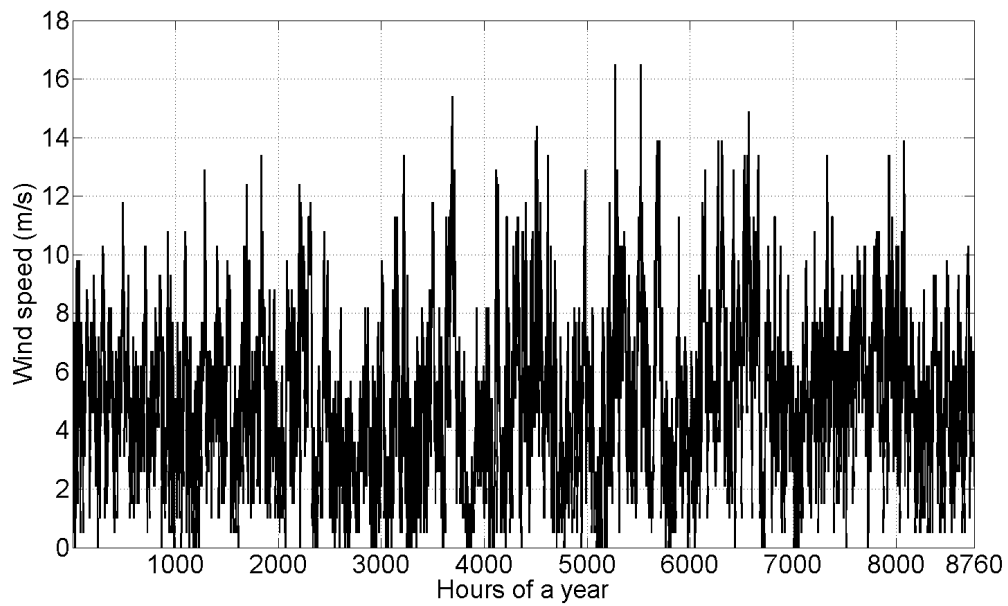


Fig. 2.2 Hourly wind speed (m/s) of a year in Auckland, New Zealand.

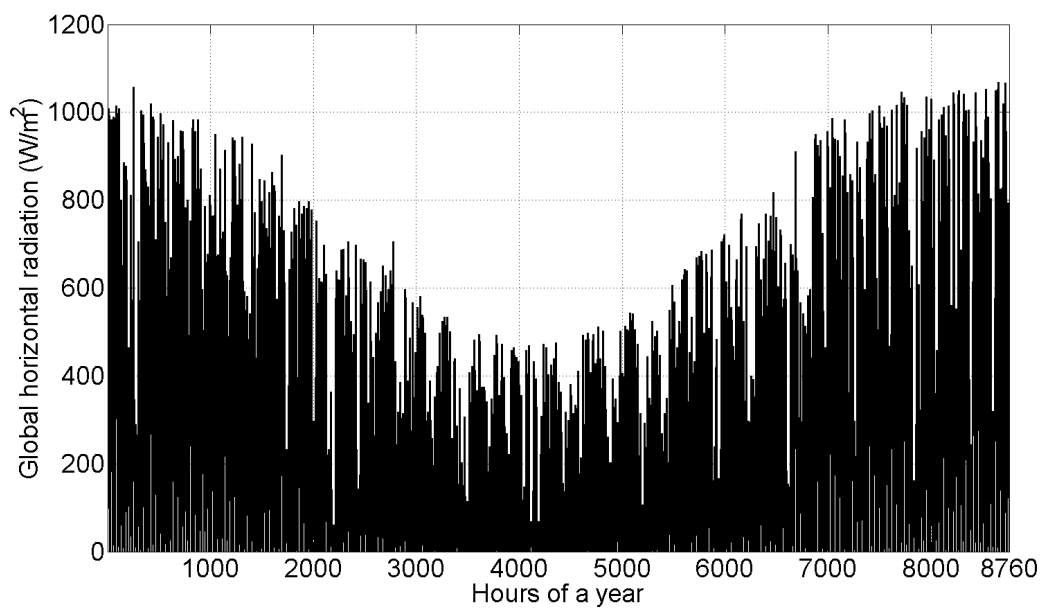


Fig. 2.3 Hourly global horizontal radiation (W/m^2) of a year in Auckland, New Zealand.

from 12:00 hr to 16:00 hr. The peak load (1.8 kW) is at 20:00 hr and it is higher than 1.5 kW from 19:00 hr and 24:00 hr. Between the hours 07:00 hr to 11:00 hr the load is above 1 kW.

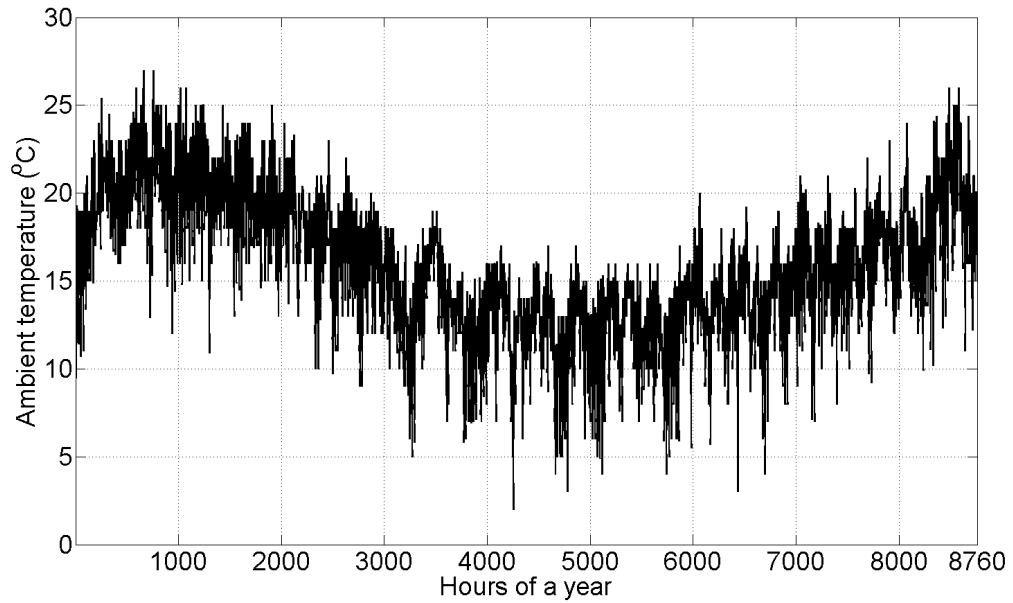


Fig. 2.4 Hourly temperature ($^{\circ}$ C) of a typical year in Auckland, New Zealand.

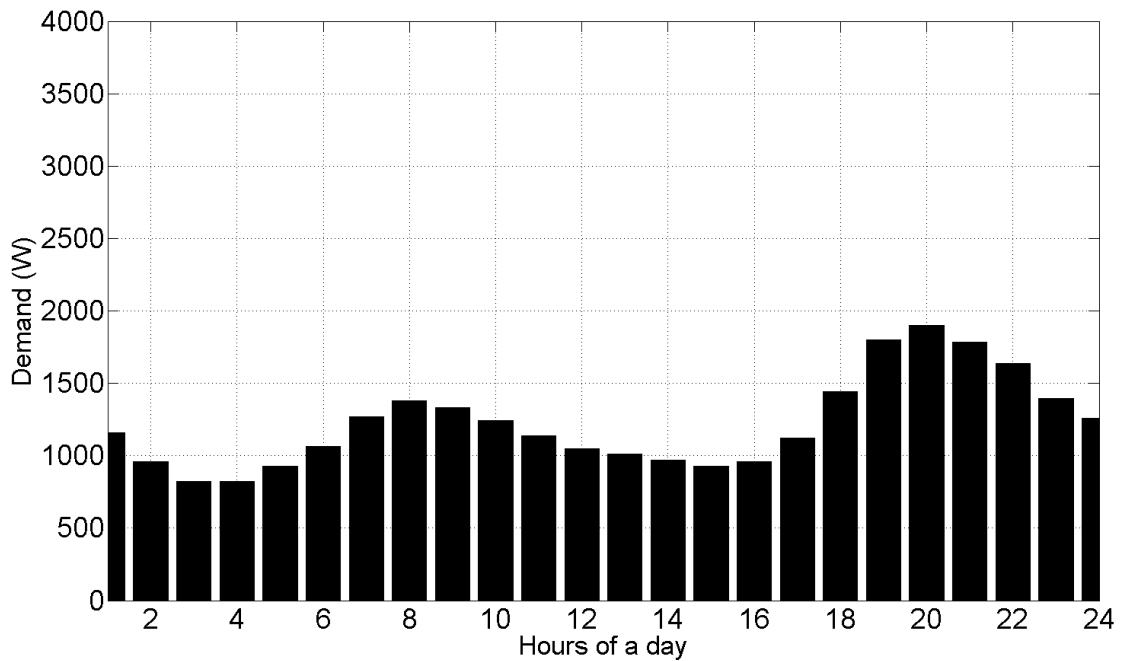


Fig. 2.5 Average hourly electrical load profile of a day.

Finally, although the weather data provides an indication of the potential output from wind and PV generators, to fully optimize a HRES it is necessary to have a characteristic model of the system. In this situation the system is made from a number of sub-components with varying individual characteristics, hence it is necessary to describe each of these individually before they are encompassed in the optimization.

2.4.1 Wind turbine generator model

When selecting a wind turbine, the manufacturer provides a nonlinear power characteristic curve for the WG that relates the wind speed and specific power output (W/m^2) from the WG. Fig. 2.6 shows a typical power characteristic curve of a WG.

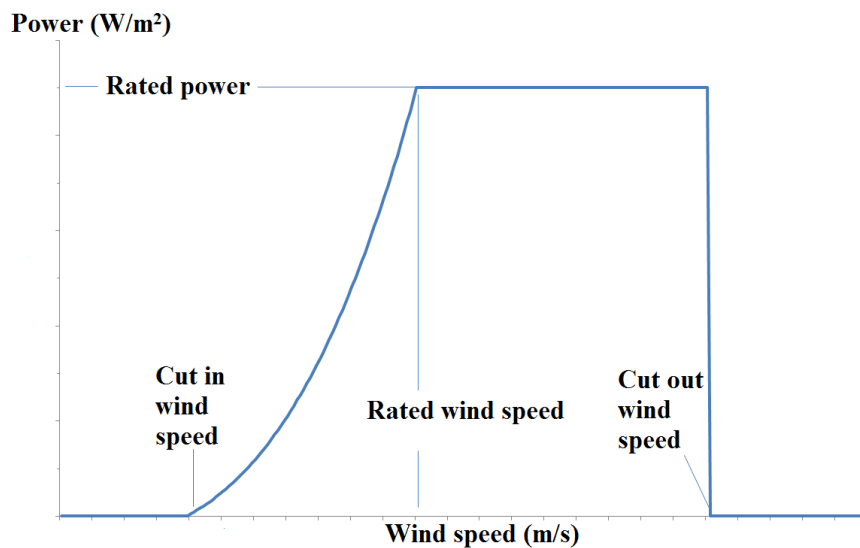


Fig. 2.6 Power characteristic of a typical wind turbine generator (WG).

However, in determining the output from the WG, it is necessary to know the wind speed at the site. The hourly wind speed of a site at a reference height (approximately 33m) can be

sourced from typical meteorological year (TMY) data and subsequently, the wind speed at any height can be calculated by equation (2.5) [63].

$$v = v_{ref} \left(\frac{h}{h_{ref}} \right)^\alpha \quad (2.5)$$

where, v_{ref} and v are the wind speed at the referenced height and the hub height respectively, and α is a power law coefficient. The value of this coefficient is less than 0.10 for very flat land, water or ice and it is more than 0.25 for a heavily forested landscape [17]. In general the one-seventh power law ($\alpha = 0.14$) is a good approximation for relatively flat surfaces such as the open terrain of grasslands away from tall trees or buildings [64] and so is used in this study.

Therefore the specific power output, $P_w(W/m^2)$ from a WG can be expressed by equation (2.6) [34].

$$P_w(v) =, \begin{cases} 0 & \text{if } v < v_{ci}, \\ av^3 - bP_r & \text{if } v_{ci} \leq v < v_r, \\ P_r & \text{if } v_r \leq v < v_{co}, \\ 0 & \text{if } v \geq v_{co}, \end{cases} \quad (2.6)$$

where, $a = \frac{P_r}{v_r^3 - v_{ci}^3}$, $b = \frac{v_{ci}^3}{v_r^3 - v_{ci}^3}$, P_r is the rated power, v_{ci} , v_{co} and v_r are the cut-in, cut-out and rated speed of the wind turbine respectively, as specified by the manufacturer.

As such, the actual electrical power from a WG can be found from equation (2.7).

$$P_{WG} = P_w A_{WG} \eta_{WG} \quad (2.7)$$

where A_{WG} is the total swept area of the WG and η_{WG} is the efficiency of the wind turbine generator and corresponding converters.

The characteristics and price of the wind turbine used in this study are shown in Table 2.1

Table 2.1 Specification of the WG

P_r (W)	V_{ci} (m/s)	V_{co} (m/s)	V_r (m/s)	h_{min} (m)	h_{max} (m)	WG capital cost (\$)	Tower capital cost (\$ per unit length)
1000	3.58	64.4	11.0	11	35	2400	35

2.4.2 Photovoltaic module model

The performance of a PV module is highly influenced by weather conditions such as solar radiation, wind speed and ambient temperature which influence the PV module cell temperature. The maximum output power of a PV module at any time can be determined from equation (2.8) [18] for the standard test conditions (STC) (cell temperature at 25°C and solar irradiance of $1kW/m^2$) given by the manufacturer, as well as the ambient temperature and irradiation conditions.

$$P_{PV}(t, \beta) = V_{OC}(t, \beta) I_{SC}(t, \beta) FF(t) \quad (2.8)$$

$$I_{SC}(t, \beta) = \{I_{SC-STC} + K_I [T_c(t) - 25^\circ C]\} \frac{G(t, \beta)}{1000}$$

$$V_{OC}(t, \beta) = V_{OC-STC} - K_V T_c(t)$$

$$T_c(t) = T_A + \left\{ \frac{(NCOT - 20^\circ C)}{800} \right\} G(t, \beta)$$

where $I_{SC}(t, \beta)$ is the short circuit current, I_{SC-STC} is the short-circuit current under standard test conditions (STC), $G(t, \beta)$ is the global solar irradiance incident on the PV module at a tilt angle of β° , K_I is the short-circuit current temperature coefficient, $V_{OC}(t, \beta)$ is the open circuit voltage, V_{OC-STC} is the open circuit voltage under STC, K_V is the open circuit voltage temperature coefficient, T_A is the ambient temperature ($^\circ C$), $NCOT$ is the nominal cell operating temperature and $FF(t)$ is the fill factor. It should be noted that under STC, the irradiance and cell temperature are taken to be $1000 \text{ W}/m^2$ and $25^\circ C$ respectively, whereas the nominal cell operating conditions are taken to have an irradiance of $800 \text{ W}/m^2$ and an ambient temperature of $20^\circ C$.

In considering this, hourly global irradiation on a horizontal plane can often be obtained from typical meteorological year (TMY) data sets. However total global horizontal radiation consists of beam and diffuse radiation so to determine irradiance on a tilted PV module it is necessary to decompose the global radiation into beam and diffuse components. The ratio of beam (G) and diffuse (D) components of this hourly global radiation can be obtained

from the hourly clearness index (k_T) expressed by equation (2.9) [65], determined by the correlation between $\frac{G}{D}$ and k_T provided in [66–68].

$$\frac{G}{D} = \begin{cases} 1.0 - 0.09k_T & \text{for } 0 < k_T < 0.22, \\ 0.9511 - 0.1604k_T + 4.388k_T^2 - 16.638k_T^3 + 12.336k_T^4 & \text{for } 0.22 < k_T \leq 0.80, \\ 0.065 & \text{for } k_T > 0.8, \end{cases} \quad (2.9)$$

Subsequently the total hourly radiation on a surface tilted at an angle β can be expressed by equation (2.10) [65].

$$G(t, \beta) = (G - D)R_b + D \left(\frac{1 + \cos\beta}{2} \right) + G\rho_g \left(\frac{1 + \cos\beta}{2} \right) \quad (2.10)$$

where ρ_g is the ground reflectance and R_b is given by equation (2.11) [65]. This assumes that the PV modules are at a fixed angle and facing true north, as New Zealand is located in the southern hemisphere.

$$R_b = \frac{\cos(\phi + \beta)\cos\delta\cos\omega + \sin(\phi + \beta)\sin\delta}{\cos\phi\cos\delta\cos\omega + \sin\phi\sin\delta} \quad (2.11)$$

where ω is the solar hour angle, ϕ is the latitude and δ is the declination.

Thus, the total power output from a PV array is given by equation (2.12).

$$P_{array}(t, \beta) = \eta_{PV} N_S N_P P_{PV}(t, \beta) \quad (2.12)$$

where N_S and N_P are the number of PV modules connected in series and in parallel respectively and η_{PV} is the efficiency of the PV modules and corresponding converters. In this study, the employed sizing optimization method determines the number of parallel connections of PV modules and the number of PV modules connected in series as defined by the bus voltage.

The characteristics and price of the PV modules used in this study are shown in Table 2.2.

Table 2.2 Specification of the PV module

V_{OC} (V)	I_{SC} (A)	V_{max} (V)	I_{max} (A)	P_{max} (W)	K_V (V/°C)	K_I (A/°C)	Fill factor	Capital cost (\\$)
64.8	6.24	54.7	5.86	320	-0.0032	0.0055	0.893	640

2.4.3 Battery model

It is assumed that the surplus electrical energy from the WG and PV would be stored in lead-acid battery banks, and energy would be extracted from the batteries when energy generated by the sources was not sufficient. The number of series connected batteries, N_{Sbat} depends on the DC bus voltage, V_{BUS} and if the nominal voltage of each individual battery is

V_{bat} , then this number is calculated using equation (2.13).

$$N_{Sbat} = \frac{V_{BUS}}{V_{bat}} \quad (2.13)$$

The capacity of the battery bank is related to the number of batteries connected in parallel and is given by equation (2.14).

$$C_n = N_{Pbat} \times C_{bat} \quad (2.14)$$

Thus, the total number of batteries can be found from equation (2.15)

$$N_{bat} = N_{Sbat} \times N_{Pbat} \quad (2.15)$$

In doing this it is important that the battery bank is not allowed to discharge fully to ensure longer battery life. In this regard the maximum permissible depth of discharge (DOD) of the battery is specified by the system designer as a percentage. The minimum permissible battery capacity during discharging is therefore given by equation (2.16).

$$C_{min} = DOD \times C_n \quad (2.16)$$

The knowledge of the real state of charge (SOC) of a battery depends on the initial SOC, the charge or discharge time and the current. The losses during the charging or discharging time and also during the storage need to be taken into account. The current SOC can be determined

from the previous SOC and the charge or discharge current as well as self-discharge of a battery. Subsequently the SOC is defined by equation (2.17) [17]:

$$SOC(t) = SOC(t-1) \left(1 - \frac{\sigma \Delta t}{24} \right) + \frac{I_{bat}(t) \Delta t \eta_{bat}}{C_{bat}} \quad (2.17)$$

where σ is the self-discharge rate depending on the accumulated charge [17], taken to be 0.2% per day as recommended by [69], and C_{bat} is the capacity of the batteries. As in [17], the depth of discharge (DOD) was set to 0.8, the battery charge efficiency (η_{bat}) was set to 0.8 and the discharge efficiency was set to 1.

Finally, the battery current of the hybrid WG-PV at any time (t) is given by equation (2.18).

$$I_{bat}(t) = \frac{P_{PV}(t) + P_{WG}(t) - P_{Load}(t)}{V_{bat}(t)} \quad (2.18)$$

where, $P_{PV}(t)$ and $P_{WG}(t)$ are the instantaneous power produced by the PV modules and the WGs respectively, $P_{LOAD}(t)$ is the demand and $V_{bat}(t)$ is the battery voltage.

Table 2.3 Specification of the battery

Price (\$)	Voltage (V)	Capacity (Ah)
1239	12	357

2.5 Reliability model based on loss of power supply probability (LPSP)

Finally, in characterizing the nature of this system, this study uses an LPSP approach. The loss of power supply probability (LPSP) is used to measure the reliability of the optimized HRES and is defined as the average fraction of a load that can not be satisfied by the system in a given time period [22] as shown in equation (2.19).

$$LPSP = \frac{\sum_{t=0}^T LPS(t)}{\sum_{t=0}^T P_{Load}(t)} \quad (2.19)$$

where, LPS(t) is the loss of power supply at hour t. The power supply can be disrupted if the demand is higher than the available power from the WG, PV modules and battery, hence the range of LPSP varies from zero to one. The load will always be satisfied with an LPSP of zero and will never be satisfied with an LPSP of one. In this research work, the probabilistic approach to LPSP calculation is incorporated with the objective function, where LPSP is defined by equation (2.20) [17].

$$LPSP = \frac{\sum_{t=0}^T \text{Loss of Power Supply Time}}{T} = \frac{\sum_{t=0}^T \text{Time}(P_{available}(t) < P_{Load}(t))}{T} \quad (2.20)$$

The loss of power supply time is the time when the available power from the renewable sources and batteries is less than the demand at that time. The available power from the

system can be found by the equation (2.21) [17].

$$P_{available} = P_{PV}(t) + P_{WG}(t) + C \cdot V_{bat} \cdot \text{Min} \left[I_{bat,max} = \frac{0.2C_{bat}}{\Delta t}, \frac{C_{bat} \cdot (SOC(t) - SOC_{min})}{\Delta t} \right] \quad (2.21)$$

Here, the available power at a time t is $P_{available}$, C_{bat} is the capacity of the batteries, state of the charge of the batteries at time t is $SOC(t)$, and C is a constant and its value is 0 for battery charging process and 1 during the battery discharging process. As the analysis is done on hourly basis, the numerical values of power is equivalent to energy.

2.6 Optimization Methodology

Among the various optimization methods, genetic algorithm (GA) and the exhaustive search technique do not require any complex mathematical calculations (derivative calculation). However, they are capable of finding optimal solutions efficiently and they were utilized for this study.

2.6.1 Genetic algorithm

Genetic algorithms (GAs) are a global optimization method and can be applied for solving a multi-variate and non-linear optimization problem such as the sizing of a HRES. The process consists of selection, crossover and mutation operations that mimic the natural evolution of

genetics [70].

Genetic algorithms are different from other optimization techniques in that they are a population based method; that is to say, they start with several probable solutions (chromosomes) at a time. These solutions may be coded with binary, real or mixed values, and the initial population is generated randomly. Thus, the solutions are scattered throughout the search space. Each of the solutions consists of multiple variables, known as the genes of the chromosome and each gene (variable) is tested against the given constraint. An objective function (for this study the 20-year total system cost) is evaluated for each of the chromosomes, provided that each gene in that chromosome satisfies the desired constraints. If the solution fails to satisfy the constraints it is then replaced with a new solution, generated randomly. The best fitted solutions are selected and sorted based on the corresponding value of the objective function. The selected solutions will be crossed among each other to get the solutions of the next generation, this is known as a crossover operation. Finally, mutation allows some of the solutions to be changed randomly to prevent immature convergence of the solution. The flow chart of the implemented GA optimization process is depicted in Fig. 2.7.

In each case, the number of chromosome was taken to be 32, natural selection rate was 0.5, crossover rate was 0.8 and mutation rate was 0.4. These parameters are selected in a way to optimize the required computation time and to prevent immature convergence. The elitist technique of the crossover operation generates a new generation of chromosome from the selected solutions except the best solution of the previous generation. As the chromosomes

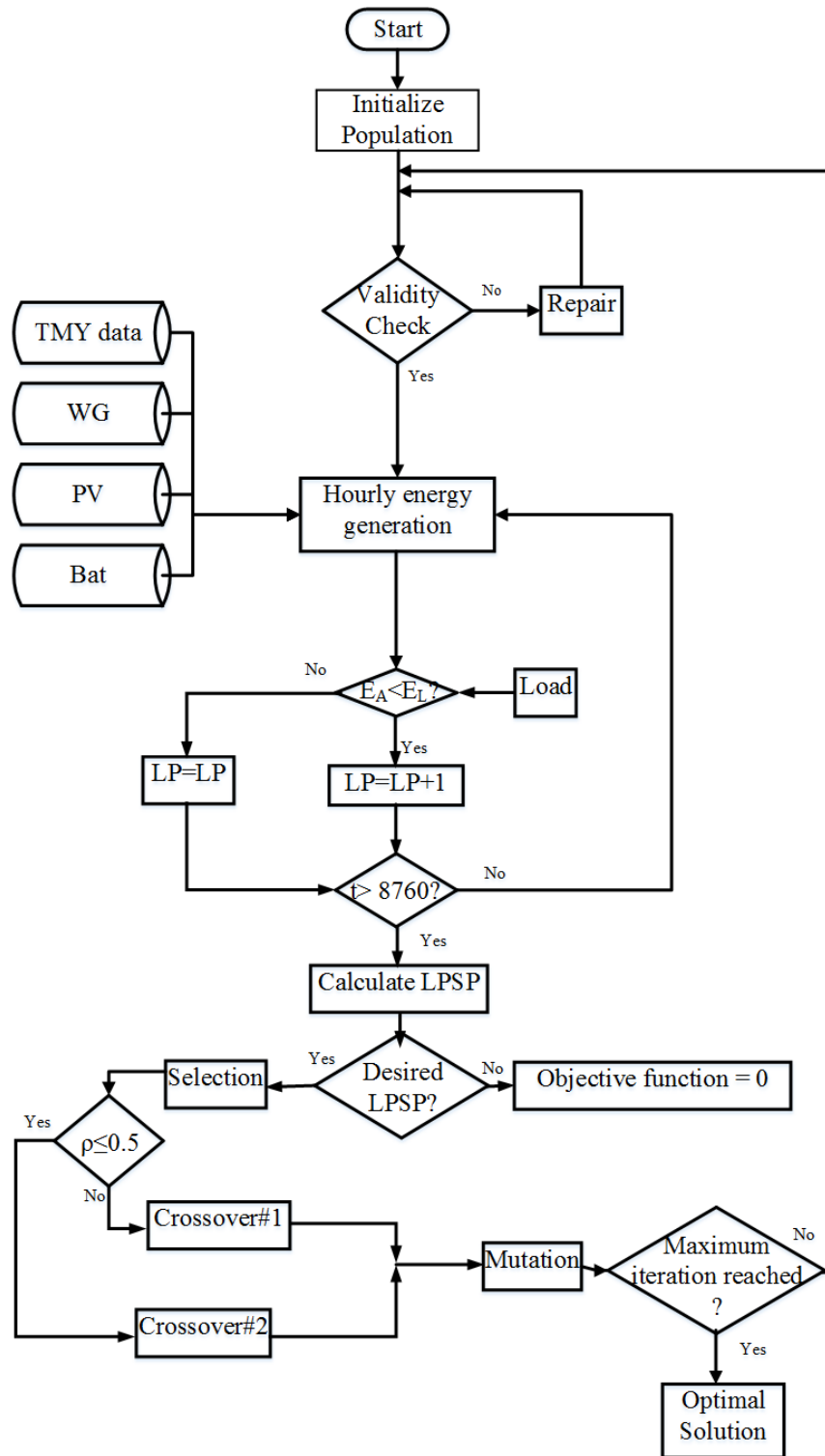


Fig. 2.7 Flow chart of the implemented genetic algorithm (GA).

converge quickly with lower mutation rates, the new generation of population due to the crossover operation may scatter within the limited search space and become trapped in local minima. The mutation rate was therefore kept higher so that the GAs could explore a much wider region in the search space. The best solution in each generation was compared with the global best and any improved result was stored as a new global best. This increased the probability of reaching the global optimum solution within a reasonable number of generations.

However, GAs are unable to guarantee the optimal sizing of a HRES within a limited number of generations as the solution may become trapped in a local optimum rather than the global optimum. On the other hand a large number of iterations require longer computation time [41].

2.6.2 Exhaustive (iterative) search method

The exhaustive search method on the other hand looks for every probable solution by linearly changing the variables within the search space. The easy to implement exhaustive search method is less likely to be trapped into local optima provided that the upper and lower bounds of each decision variable are selected correctly. However, it requires a large number of iterations that increase the computation time, or the optimal size may be trapped into local optima due to the selection of searching space. In most previous studies using exhaustive search methods the number of variables was thus limited to only three. However, the number of variables can be increased by reducing the searching space and by selecting upper and

lower bounds of variables within a reasonable ranges. Fig. 2.8 shows the flow chart of an iterative method.

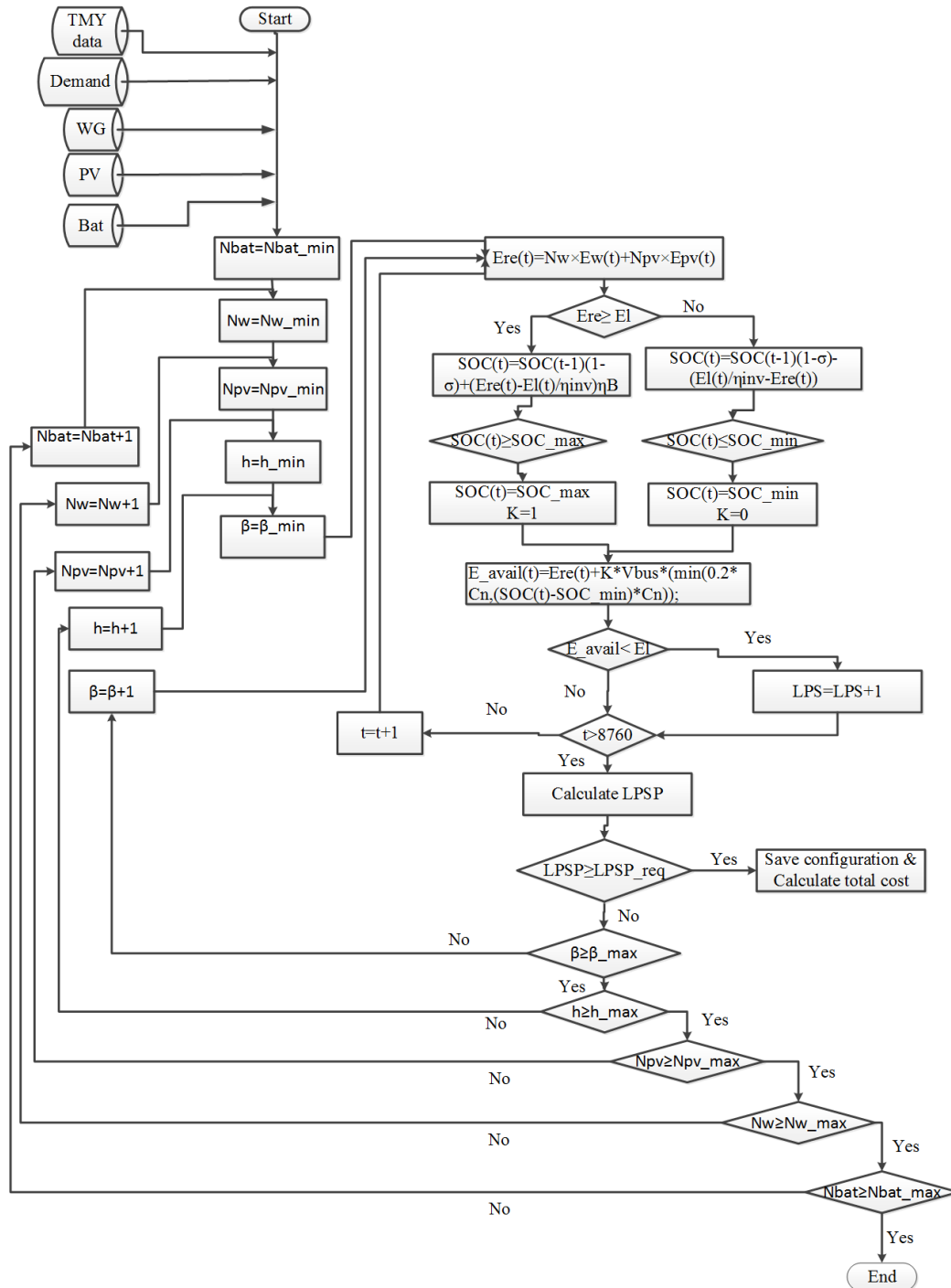


Fig. 2.8 Flow chart of the implemented exhaustive search (iterative) method

2.6.3 Hybrid (GA-exhaustive search) optimization method

It is noted that the exhaustive search technique and the GA global optimization method, require a large number of iterations in order to converge to the optimal size of a HRES. Furthermore, stochastic GA methods are unable to guarantee an optimal solution even with a large number of generations [41]. Thus, a hybrid method has been implemented and utilized for sizing a HRES throughout this work. The method utilizes the advantages of both GA and the exhaustive search technique thereby eliminating the drawbacks associated with each individually.

A key property of a GA is that it converges quickly to the approximate optimal solution, this property is exploited to define the bounds of the decision variables. Several runs of only 300 generations of a GA are used for this purpose. Each run of this limited generation of GA closely approximates the optimal size of a HRES and confines the search space. Subsequently the exhaustive search technique is employed to find all combinations within the bounds that satisfy the desired reliability index, LPSP. The combination with the lowest life-time cost is taken as the optimal size of the HRES for the given demand. As the searching space of the iterative method can be reduced by the GA, the PV module tilt angle (β^o) and the WG installation height (h) can also be included in the decision variables. The flow chart of the implemented hybrid optimization method is shown in Fig. 2.9.

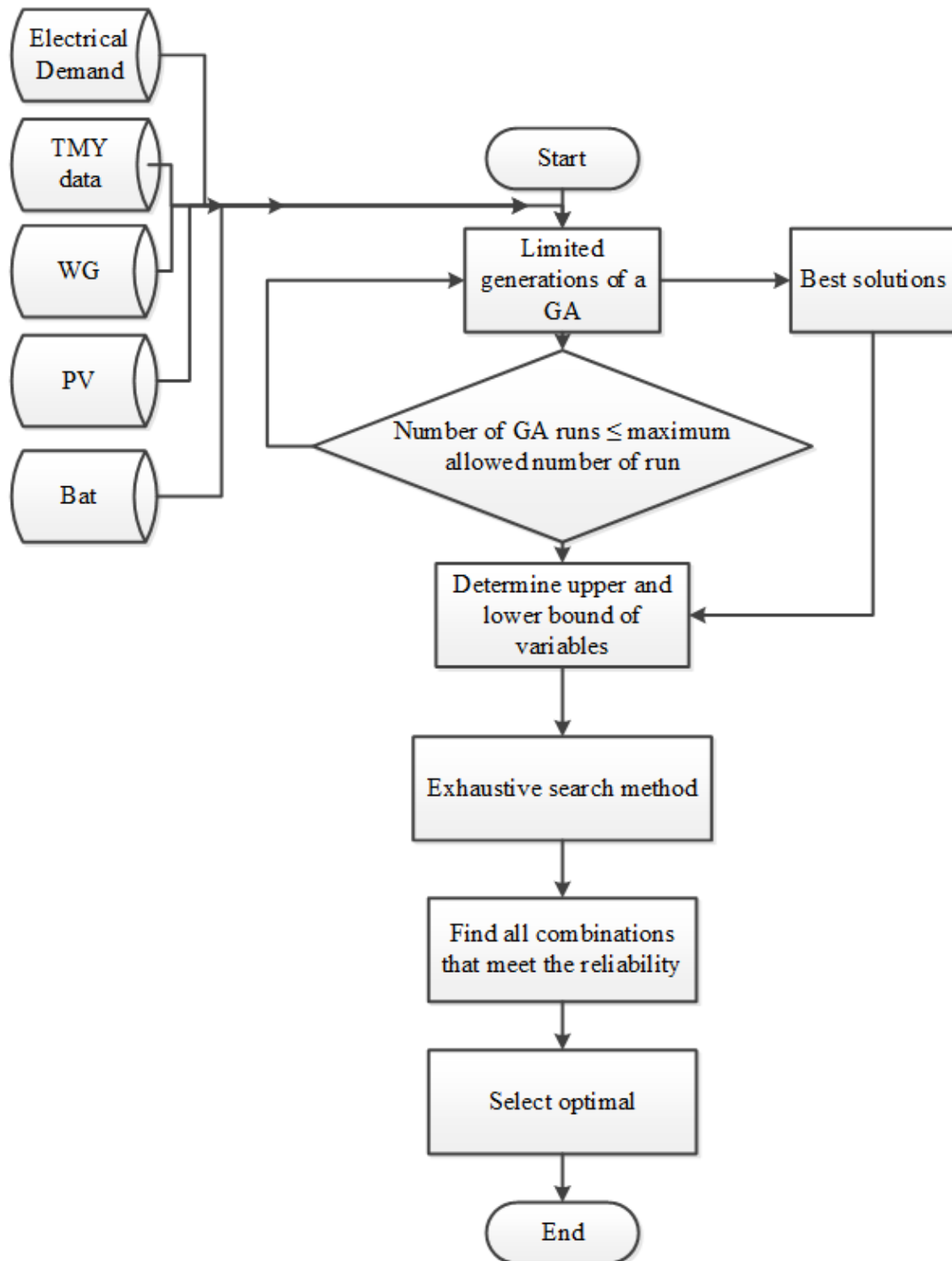


Fig. 2.9 Flow-chart of hybrid optimization method

2.7 Results and Discussion

2.7.1 Optimal size of a HRES for typical annual demand profile

In order to validate the method, a HRES was sized for the average electrical load profile as shown in Fig. 2.5 using the hybrid optimization method and the result obtained was compared with the result of a GA. The annual hourly demand profile consisted of the daily electrical demand repeated everyday throughout the year.

To do this the GA was run for 300 generations only and the size of the HRES was approximated. Several approximate optimal sizes of a HRES resulting from 300 generations of a GA are shown in Table 2.4.

Table 2.4 Approximate result with 300 Generation of a GA

WG #	PV #	Battery #	Height (m)	Tilt angle (°)	Total cost (\$)
7	69	16(8 × 2)	17	60	297,998
18	68	14(7 × 2)	19	58	310,795
12	72	14(7 × 2)	17	65	290,791
5	90	14(7 × 2)	32	34	282,607
11	75	14(7 × 2)	15	68	288,577

The approximate optimal sizes as shown in Table 2.4 were used to determine the bounds of the decision variables using one of the following methods.

Method I: Among the sizes in Table 2.4, the optimal solution was assumed to be around the

size of the lowest total system cost. Thus, the bounds of the decision variables was taken to be around the size of the lowest system cost shown in Table 2.5.

Table 2.5 Defining the bounds of decision variables using method I

Variable	Min	Max
N_{WG}	4	6
N_{PV}	70	110
N_{Bat}	12(6 × 2)	16(8 × 2)
β	20	60
h	20	35

Method II: In this method, the bounds were selected based on the minimum and maximum values of the decision variables resulting from the approximate optimal sizes of a HRES suggested by the GA. Table 2.6 shows the minimum and maximum values of the variables as found from the limited generation of GA.

Table 2.6 The minimum and maximum values of the variables as found from the limited generation of GA

Variable	Min	Max
N_{WG}	5	18
N_{PV}	68	90
N_{Bat}	14(7 × 2)	16(8 × 2)
β	34	68
h	15	32

Thus, the upper and lower bound was taken as shown in Table 2.7.

Table 2.7 Defining the bounds of decision variables using method II

Variable	Min	Max
N_{WG}	4	19
N_{PV}	65	75
N_{Bat}	$14(7 \times 2)$	$16(8 \times 2)$
β	30	70
h	15	35

With the upper and lower limits of the decision variables defined, the exhaustive search method can find all the feasible combinations within 123,984 iterations using method I and 303,072 iterations using method II. Thus, the hybrid optimization requires only 133,584 and 312,672 iterations with method I and method II respectively. This provides a significant reduction in iterations compared to the exhaustive search method (2275×10^6).

Though, the number of iterations performed is comparable with the GA, GA requires longer times and is unable to guarantee the optimal solution with such a large number of iterations.

As further validation of the method, the optimized size of the HRES obtained by the hybrid (GA and exhaustive search) method was cross referenced with the solutions obtained by a GA alone as shown in Table 2.8.

Table 2.8 Optimal size of a HRES using hybrid method and GA for the average load profile of Fig. 2.5

Method Name	WG #	PV #	Bat #	Height (m)	Tilt angle ($^{\circ}$)	Total Cost (\$)
GA	6	75	14 (7 × 2)	32	54	275,310
Hybrid	6	75	14 (7 × 2)	32	54	275,310

2.8 Concluding remarks

It is apparent that both these methods provide the same size HRES for the given load profile, thus demonstrating the capability of a hybrid optimization method. However, as the hybrid optimization method obtained can guarantee the optimal size with a limited number of iterations.

Now in considering the results of this optimization, it is important to note that the daily demand profile typically depends on various factors such as user actions, internal and external household temperature and the socio-demographic factors of the inhabitants. Thus, the optimized size considering the daily demand of a single day to be repeated throughout the year may be unable to meet the demand with desired reliability as affected by these factors. Therefore, the work following on from this benchmark optimization examines how such factors can influence the sizing of a HRES.

Chapter 3

Optimal Sizing of a HRES Considering Socio-Demographic factors

3.1 Introduction

Each device of a stand-alone hybrid renewable energy system (HRES) needs to be selected and mixed optimally in order to make the system reliable and cost effective. The time varying user demand, the non-linear system characteristics and uncertain generation from WG and PV modules make the size optimization of a HRES more complicated. Thus the demand profile of a site is of great importance as it dictates the size of the system components. However, for many applications, particularly residential dwellings, this load is generally stochastic in nature and governed by a wide range of internal and external factors such as the socio-demographic characteristics of the household occupants and also seasonal variations [61]. Socio-demographic characteristics usually refer to age, sex, place of residence, religion,

educational level, marital status, household status, interests, values, social groups and working patterns. Though climatic factors are mainly responsible for the variation of energy load profiles of most houses [61], socio-demographic factors of the occupants of a house also affect demand profiles considerably.

Numerous load profiles have been used in sizing HRES, however, none of these approaches considered the socio-demographic factors and their effect on the sizing a HRES. In [22] the seasonal variations were considered in sizing PV modules and batteries for a given WG and desired loss-of-power-supply-probability (LPSP) and [23] presented a graphical construction method for determining WG swept area and PV module area for winter and summer seasons. Weekend and weekday loads were taken into consideration in [38] in order to include the effect of the working pattern of the residents while sizing a HRES. In [59] six different demand profiles were considered while using fuzzy logic for sizing a HRES. The demand profiles included midday and midnight peak of summer and winter load, as well as constant summer and winter demand, in order to consider the same and varying annual electrical load.

Now, [61] undertook a wide ranging study on household energy use in 40 New Zealand houses and noted that the demand profiles of a site as a result of the socio-demographic factors, could be classified into six different classes. In this chapter, the average daily load profiles of each class are investigated for their influence on the optimal sizing of a HRES using the hybrid optimization method consisting of a GA and exhaustive search method

described in chapter two. From this analysis, the optimally sized systems considering socio-demographic factors are suggested.

3.2 Demand profile

As mentioned earlier, an average daily profile of 40 houses developed from an average one-month's data was analyzed in [61] for determining generic daily electrical demand profile. Those profiles were classified into six classes using a Kohonen probabilistic neural network [71]. This network defines its own criteria that allows the user to set the number of classes and some of the learning parameters while classifying patterns [61]. Figs. 3.1-3.6 show the six demand profiles identified from this study, each of which is the average of its class. An examination of these six profiles reveals that each of them is markedly different from the others both in temporal position and amount of energy use. This is due to the effect of socio-demographic factors, even though they are only the average for each of the classes.

The profiles are identified as follows:

Class #1: High night use

The energy consumption as shown in Fig. 3.1 is very high over night with a low consumption during the day and medium in evening. This indicates that the consumers of this profile are particularly active at night. The energy use increases from 24:00hr and continues to 07:00hr with a peak demand of about 3700 W. The occupants of this type of household are quite possibly young and working people who remain outside during the day and come back at

different times at night. The profile suggests that the occupants remain active for several hours at night. This may also correspond to weekend energy consumption in a house where occupants start their activities in the evening, and the whole day they are either sleeping or remain outside. The consumption may be due to cooking, having hot showers, watching television, using washing machine or drier.

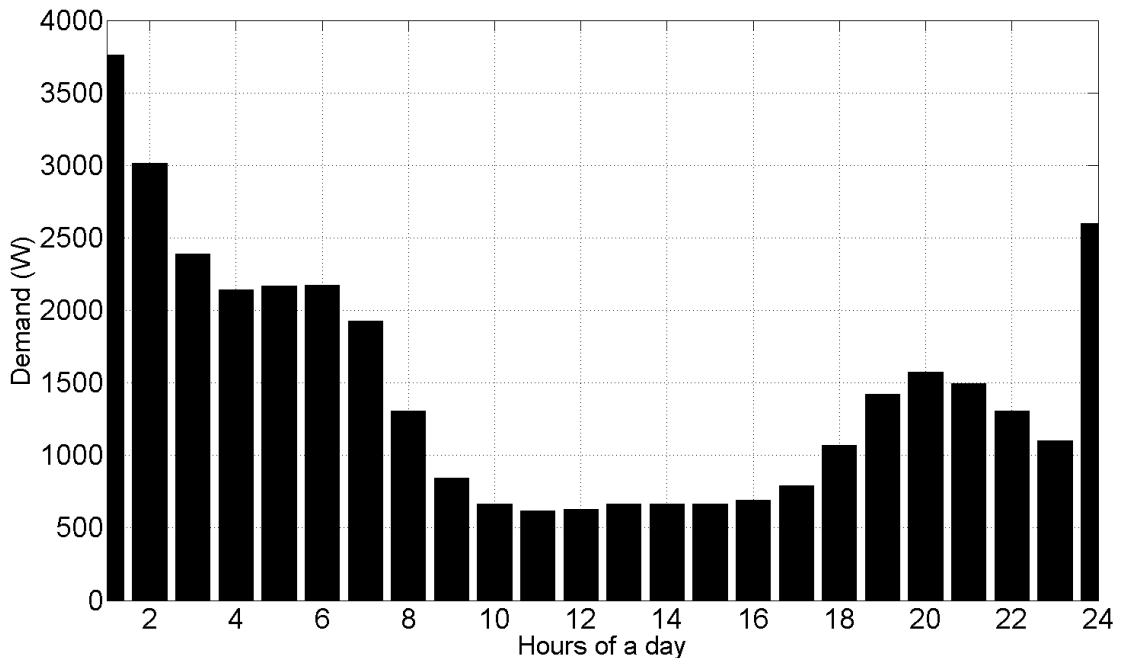


Fig. 3.1 Demand profile of Class #1 (high night use).

Class #2: Similar morning and evening peak with low midday use

This profile as shown in Fig. 3.2 is characterized by a similar morning and evening peak load. The consumers of this profile are likely working persons who go to work in the morning and come home in the afternoon. The residents of this house are likely a working couple or family with school aged children, as the low day usage suggests they remain outside during

typical working hours of the day. The hot water shower, cooking appliances and television might consume most of daily energy consumption during morning and evening.

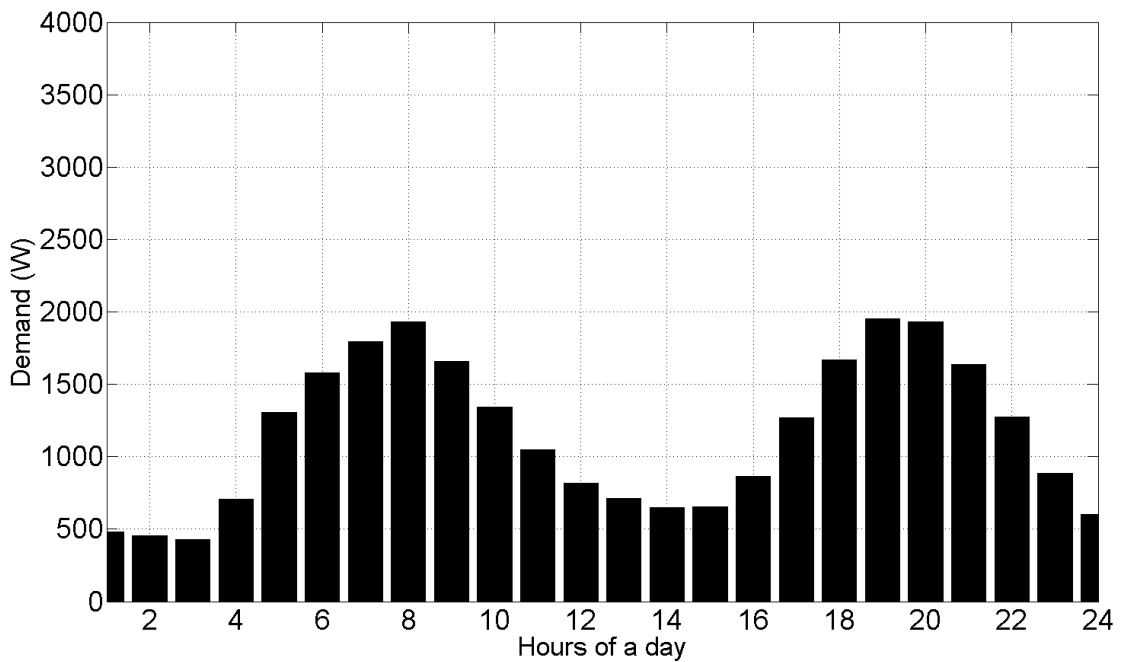


Fig. 3.2 Demand profile of Class #2 (Similar morning and evening peak with low midday use).

Class #3: High day use with morning peak

The occupants of the houses of this profile has a relatively constant electrical energy demand all day long. The profile of Fig. 3.3 shows slightly high usage profile in the morning and early evening that may be due to cooking and showers. The energy consumption profile suggests that the occupants of this house are active and present in the house all day and may work from home.

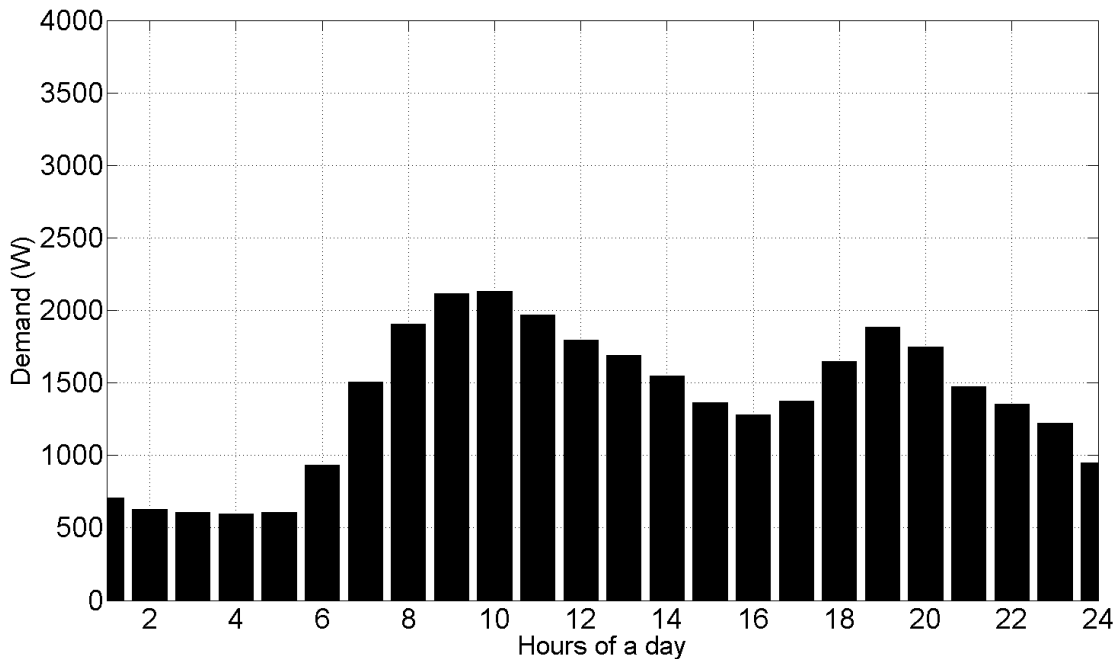


Fig. 3.3 Demand profile of Class #3 (high day use with morning peak).

Class #4: Extended evening peak

The profile as shown in 3.4 is characterized with the electrical demand extended for a longer period in the evening. The demand has a comparatively low and short morning peak suggesting the residents take showers in the evening. The occupants of this house may be a couple or a family with children. The consumption peak at 20:00 hr and 21:00 hr may be due to energy consumption from several televisions, video recorders and may also include hot water showers after returning from jogging or exercise. The high energy consumption at peak hours indicates their status and ownership level of different electrical equipment.

Class #5: Medium flat day use with early evening peak

The load profile of this class as shown in Fig. 3.5 shows an increase in energy consumption

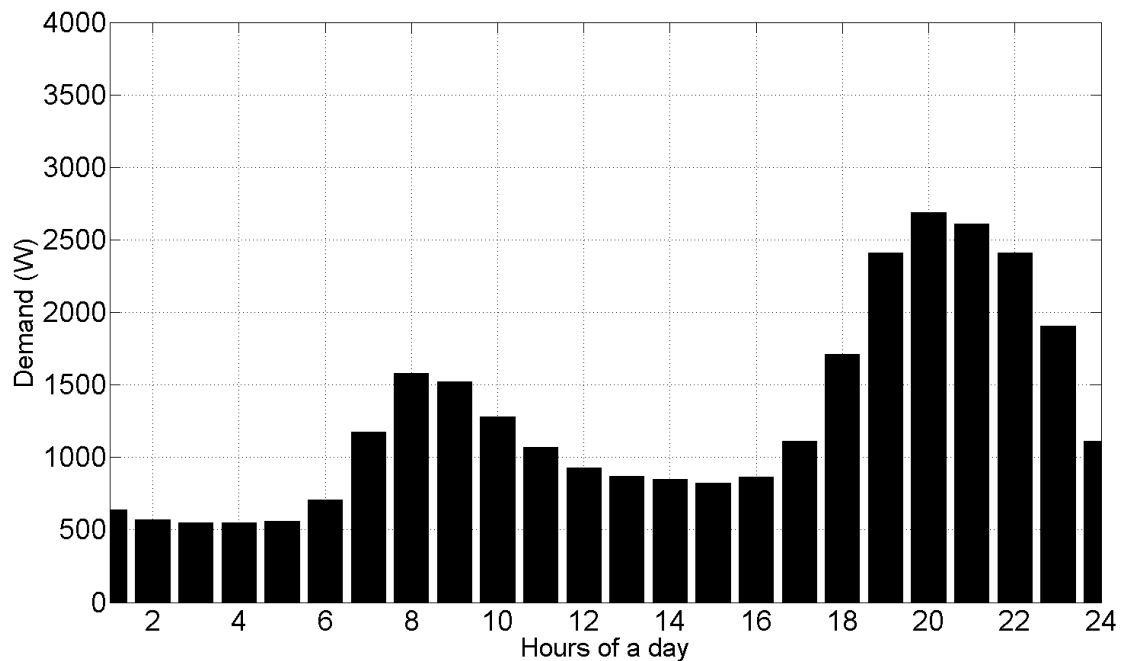


Fig. 3.4 Demand profile of Class #4 (extended evening peak).

during the day and early evening. The largest energy consumption is in between 16:00 hr and 23:00 hr. This suggests that the residents of these profile user remain active during the day. The energy consumption profile suggests that retired people are likely to live in the house as the profiles in this class are similar due to similar social status [61]. Almost 80% of its component profiles are from those of the houses where the occupants' have similar main income.

Class #6: Low use with evening peak

This profile as shown in Fig. 3.6 is similar to class # 5. Energy consumption is even lower during day and having late evening peak. This suggests that a few of the occupants are remain at home during the day and they may cook, take showers, watch television or work

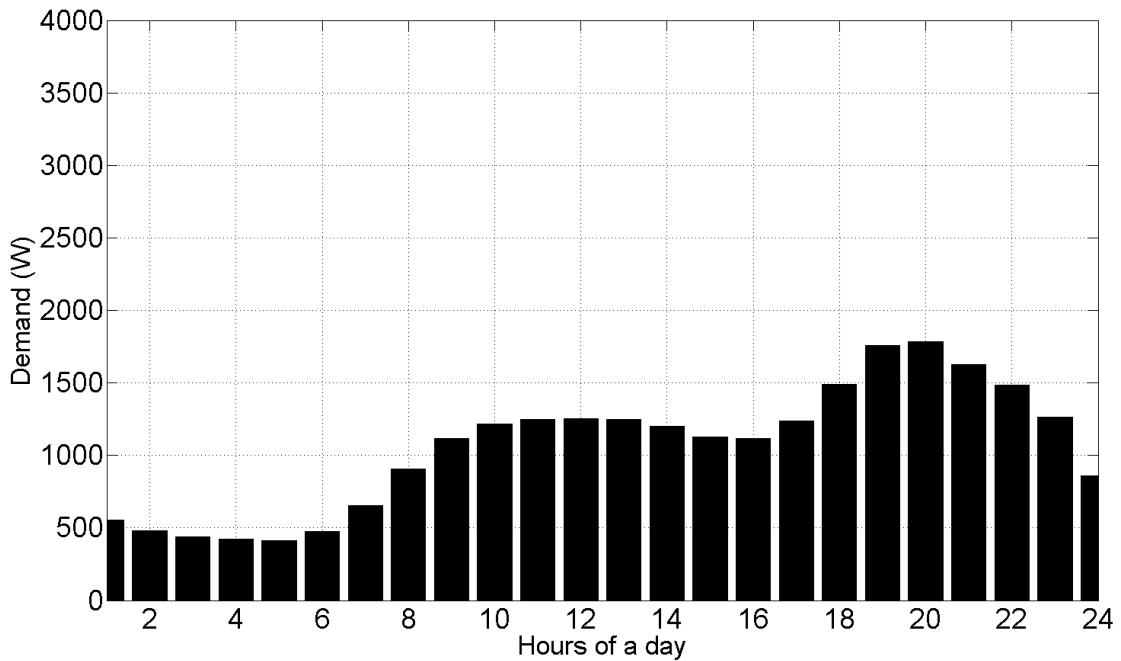


Fig. 3.5 Demand profile of Class #5 (medium flat day use with early evening peak).

with computers during the evening period.

Each of the demand profiles for these six classes are unique in terms of their hourly energy consumption and their temporal distribution. Based on these six classes, it is possible to illustrate the effect of socio-demographic factors on the optimal sizing of a HRES, as the profiles are influenced by these factors. As the peak demand magnitude varies significantly for each of the classes, the optimization was attempted for the average of each profile class and average of these six profile classes using the hybrid GA/exhaustive search method described previously, optimization was performed for a HRES operating with each class of users demand profile repeated across the year.

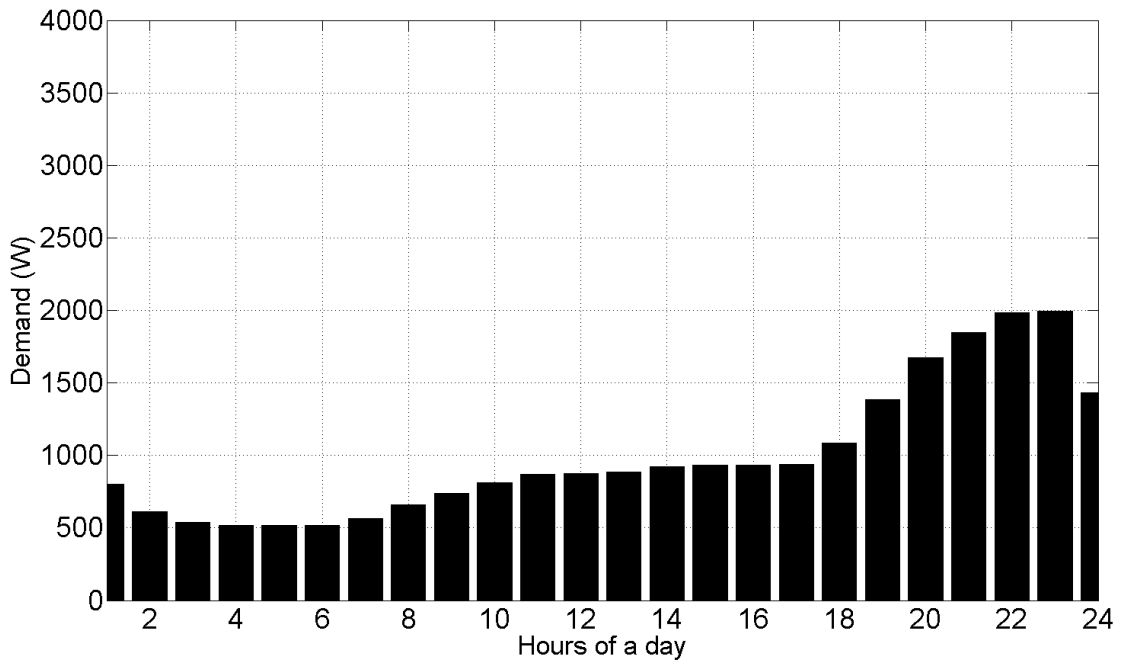


Fig. 3.6 Demand profile of Class #6 (low day use with evening peak).

3.3 Results and discussion

3.3.1 Optimal size considering socio-demographic factors

To explore the effect of socio-demographic factors, each of the load profiles shown in Fig. 3.1 to Fig. 3.6 were used for optimal sizing a HRES with zero LPSP. The results are shown in Table 3.1.

An analysis of these results shows up several important considerations regarding the optimal size of a HRES and the demand profile. It can be seen that the optimal size for the “overall low use” profiles (class #5 and #6) is almost the same due to the similarity in magnitude and distribution of the load.

Table 3.1 Optimized size of a HRES for each of the profile classes

Load Profile	WG #	PV #	Battery #	Height (m)	Tilt angle ($^{\circ}$)	Total Cost (\$)
Class #1	8	97	18 (9 × 2)	29	50	354,609
Class #2	4	77	14 (7 × 2)	29	45	267,895
Class #3	6	95	14 (7 × 2)	34	27	291,175
Class #4	4	110	14 (7 × 2)	30	20	293,407
Class #5	4	65	12 (6 × 2)	28	50	231,798
Class #6	4	62	12 (6 × 2)	29	51	228,894
Avg.	6	75	14 (7 × 2)	32	54	275,310

However, the “high extended evening peak” profile (class #4) has a distinct morning peak, low midday and a high evening peak demand extending from 18:00 hr to 24:00 hr. The outcome of this is that the number PV modules for this class increases significantly from the “overall low use” profile classes, as does the requirement for battery storage. On the other hand, the “high day use with morning peak” profile exhibits a flat high day use. A large morning peak that gradually reduces through the afternoon, before a moderate evening peak. This causes a significant change in the proportion of both WGs and PV modules in the optimum sizing, as the solar radiation in the early morning and evening is low, meaning the demand is satisfied with an increased number of WG. A similar outcome is also observed in

case of “high night use” profile (class #1), where the loading is principally night based, with low loading during the day.

Thus, it is clear from the analysis that higher evening and night demand requires more WGs whereas higher morning and midday demand are satisfied by increasing the number of PV modules. To illustrate this point further, Pearson’s correlation between hourly load and the average hourly solar radiation and wind speed for each class of demand profiles was calculated and presented in Table 3.2. The values can be varied from +1 to –1. The value of +1, 0 and –1 indicate strong positive correlation, no correlation and strong negative correlation respectively.

Table 3.2 Pearson's correlation coefficient between average hourly solar radiation and wind speed with each of the demand classes

Load Profile	Pearson’s coefficient with solar radiation	Pearson’s coefficient with wind speed
Class#1	–0.735	–0.736
Class#2	–0.253	–0.149
Class#3	0.536	0.460
Class#4	–0.277	–0.108
Class#5	0.278	0.465
Class#6	–0.211	–0.042

It is evident from the Pearson’s correlation coefficient values that the “high night use (class #1)” demand profile shows a strong negative correlation with the solar radiation and wind speed of the site. From this it can be inferred that, for heavy night usage the storage size needs to be increased significantly to meet the load, as was borne out by the optimization.

On the other hand, for loads exhibiting a positive correlation, such as the “high day use with morning peak (class #3)” profile, the solar and wind require less storage capacity as the instantaneous generation can satisfy much of the demand.

The key consideration of optimizing a HRES based on socio-demographic factors is in understanding how a system sized for one class of users responds to the demands from another class of users, for instance if there is transfer of ownership of the system. Therefore, a cross comparison of the LPSP was undertaken for each system operating with other load profiles as shown in Table 3.3.

Table 3.3 Cross LPSP results for each sized HRES

System for Profile	LPSP(%) for					
	Class #1	Class #2	Class #3	Class #4	Class #5	Class #6
Class #1	0.00	0.00	0.00	0.00	0.00	0.00
Class #2	1.83	0.00	0.39	0.27	0.00	0.00
Class #3	0.57	0.00	0.00	0.01	0.00	0.00
Class #4	0.50	0.00	0.01	0.00	0.00	0.00
Class #5	3.97	0.32	2.11	1.78	0.00	0.00
Class #6	4.52	0.55	2.72	2.28	4.00	0.00

It was found that only the optimized system for “high night use” profile could provide a zero LPSP for all loading conditions. However, such a system significantly increases the cost by trying to satisfy the highest night use and lower day use profile compared to the cost of other classes. Conversely, the optimized size for classes #3 and #4 shows good performance in meeting the conditions of all classes with moderate system cost.

3.3.2 Reliability and system cost analysis

The reliability and the system cost are two important concerns in determining the optimal size of a HRES. Thus, the system cost increases significantly as the reliability of the system is increased. To illustrate this point, the daily demand of class#1 is examined by the duration and the level of demand as shown in Fig. 3.7. From this it can be seen that the peak demand extends for only one hour during the day and the second highest load for two hours of the day while a base load of approximately 600W only remains throughout the whole day. Taking this further, from Fig. 3.8 it is evident that the state of charge (SOC) of the optimal size battery approaches its minimum SOC only once in a typical year, between the year hours of 4210 and 4230. This is due to the fact that the renewable generation through this period is low relative to demand.

The low renewable generation and higher demand only for a short duration of the year increases the size of the system while the available energy is much higher than the demand in the rest of the year. Thus, the excess energy is wasted throughout the year and the utilization

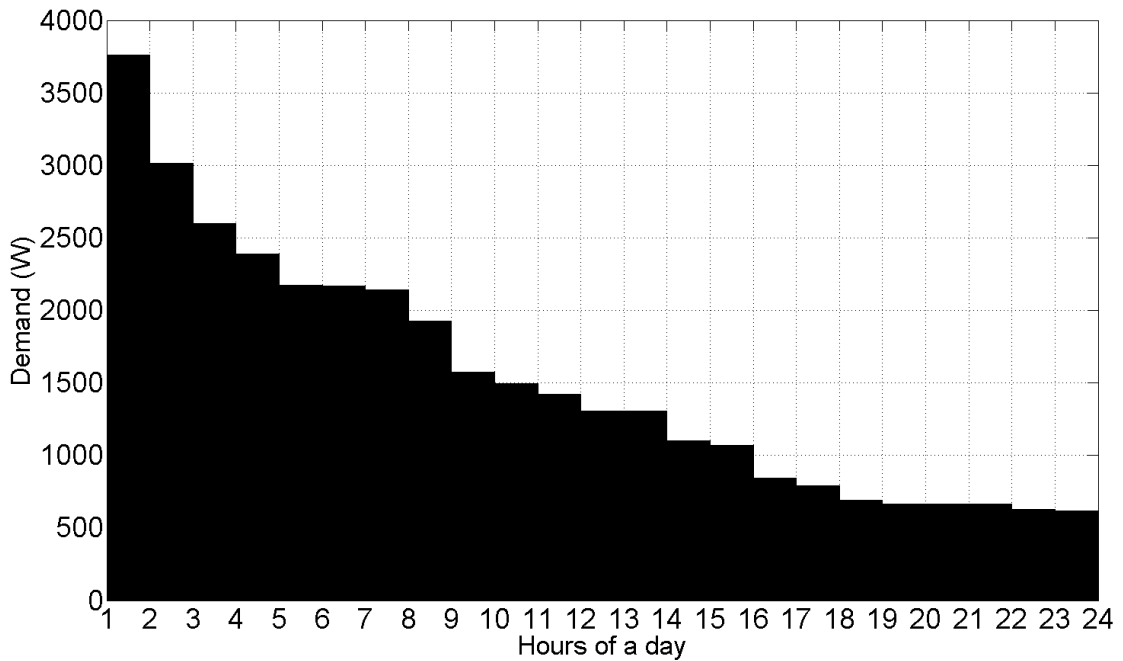


Fig. 3.7 Level and duration of the demand of a day.

factor of the system is low. In order to better understand this, the total system cost was analyzed against different values of the LPSP. Hence, a system was sized for the profile of class#1 where the value of LPSP was allowed to vary from 0% to 1%, the results shown in Fig. 3.9 illustrate that a significant reduction in life time costs can be achieved with only a small increase in the LPSP. It is further noticed that the optimized system for “high night use” demand profile with 0.25 percent LPSP provides minimal unmet demand to all the classes and the total cost is also comparable with the system optimized for high day use with morning peak and high extended evening peak demand profiles. The battery SOC for 0.25 percent of LPSP is shown in Fig. 3.10.

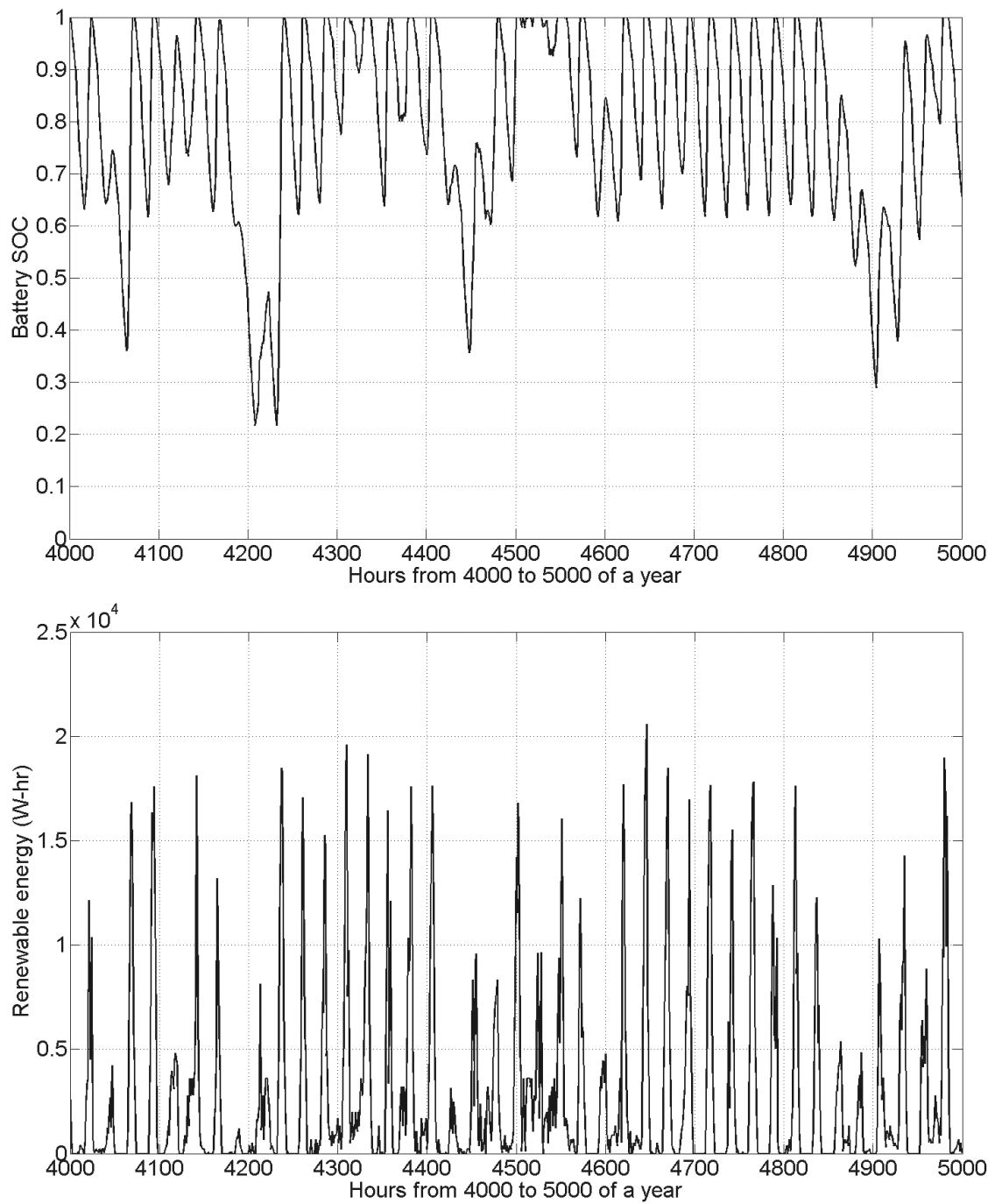


Fig. 3.8 Variation of battery SOC and generated renewable energy from 4000hrs to 5000hrs of a year.

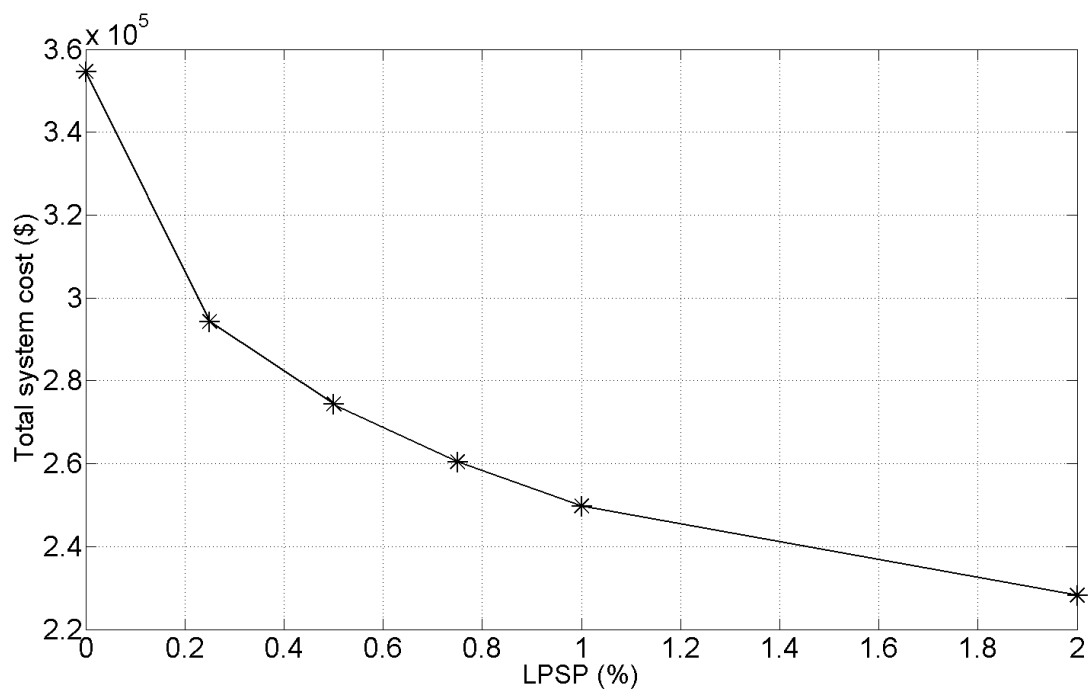


Fig. 3.9 Total system cost variation with the change of LPSP.

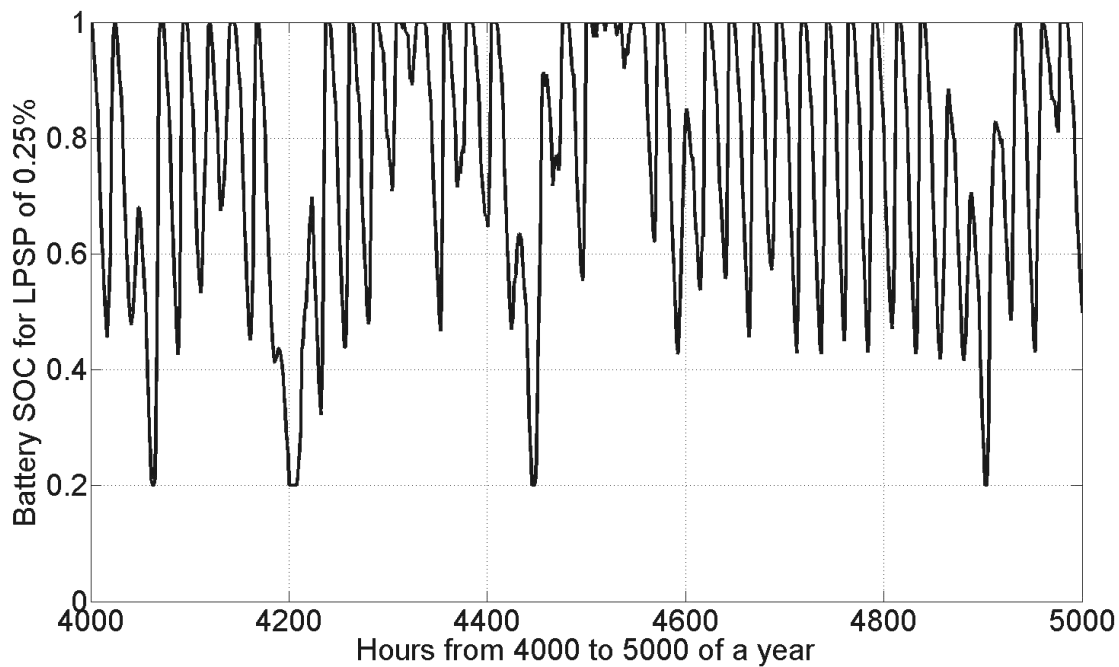


Fig. 3.10 Variation of battery SOC for LPSP of 0.25 percent.

3.4 Concluding Remarks

In this chapter socio-demographic factors of a HRES site were examined to determine their influence on the optimal size of a WG, PV module and battery HRES. Six profile classes were identified and utilized for considering these factors. Moreover, it was found that the optimal size for one class profile either can not satisfy the other class profiles with zero LPSP unless the system becomes large and therefore costly. In this respect the cost is influenced significantly by the magnitude and temporal positions of the peak demand. Furthermore, the temporal position and duration of the peak demand should be taken into account in order to find the optimal size of HRES. In this regard, the electrical demand variation due to socio-demographic factors should be integrated to sizing a HRES.

Thus, it is suggested that the HRES size that minimizes the total system cost as well as the unmet demand with all the classified socio-demographic load profiles of the site for a desired reliability can be considered as an overall optimum. However, by optimizing based on socio-demographic profiles the system cost can be reduced.

Chapter 4

Optimal Sizing of a HRES under Time

Varying Load

4.1 Introduction

In the preceding chapters an optimization was performed for a HRES with a fixed daily load repeated across a full year. In reality though the demand of a site is usually somewhat stochastic in nature and typically loads vary both in magnitude and temporal position due to variation of the user's day-to-day actions as well as seasonal variations. Domestic electricity load profiles are usually cyclical and are shaped by the individual electrical appliance. However, the switching on and off of any electrical appliances is usually influenced by various environmental, dwelling and occupant characteristics. Therefore, an electrical load profile can be described as the combination of deterministic and stochastic processes [42]. The electrical demand at any time can be assumed to be a combination of four separate

components: the normal part, the weather sensitive part, the special event part and a random part [47]. The base load in the profile usually remains constant and continues throughout the year and is dependent on the use of cold appliances. The later three parts of the power demand are defined by the user activities and environmental effects and the base demand [72] while the peak demand of the profile is usually due to the random and weather sensitive parts.

In this regard, a 30 percent day to day load variation was considered by [37] when sizing a wind-PV-diesel generator hybrid power system. In [73] six different demand profiles and weekend and weekdays demand profiles [58] were considered in optimal sizing a HRES. However, the random variation of magnitude and temporal position of peak values in stochastic annual demand profile were not considered in previous studies and it was suggested that this is common in real life demand profiles. In this chapter of the work, it is thus intended to examine the effect and the size of a HRES under time varying demand.

4.2 Demand profile

As this work aims to examine the effect of random variation both in magnitude and temporal position on the optimal size of a HRES, the average daily winter and summer load for a single household in Auckland [74] as shown in Fig 4.1 was examined. From these two time slots from 07:00 hr to 12:00 hr and 16:00 hr to 21:00 hr were identified based on the temporal position of the peak demand. During these times, the hourly loads were assumed to randomly

vary by $\pm 25\%$. Further it was assumed that the load of any individual hour could change its temporal position within the identified time slots. This is due to the fact that on average users activities are broadly similar within a period of a day, but most likely not identical. Outside these time slots, the load was assumed to remain fixed assuming these as the normal part of the electrical load profiles.

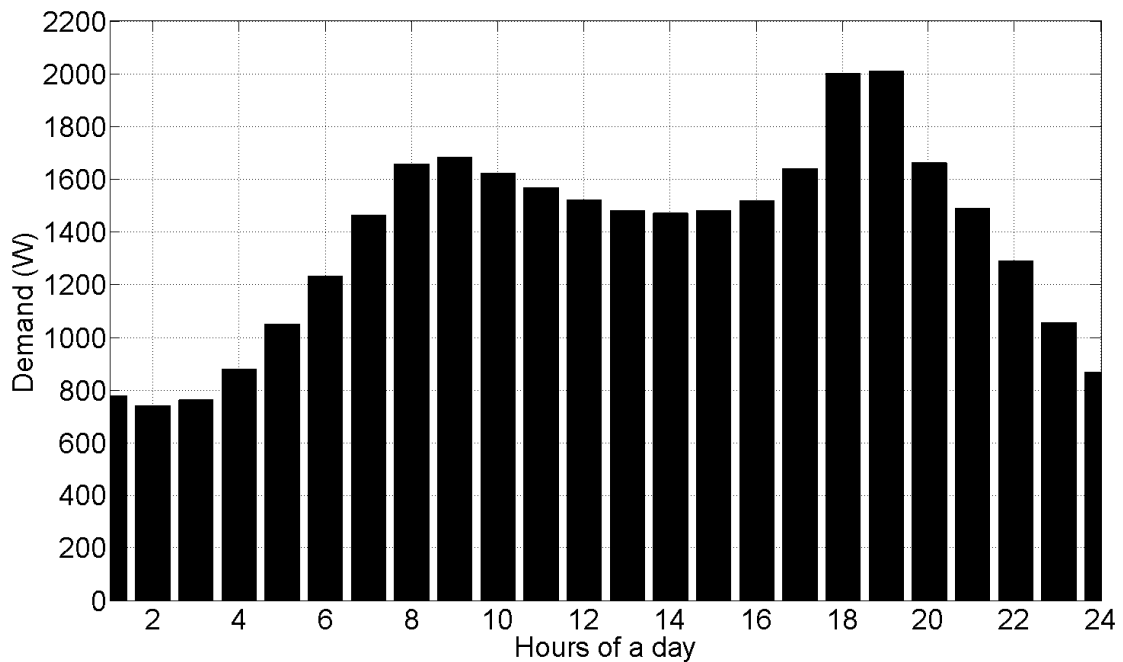


Fig. 4.1 Hourly electrical load profile of a day.

4.3 Sizing Methodology

If an annual demand profile can be used to optimize the size of a HRES that can satisfy any randomly varied profiles then the annual demand profile is considered to be a critical combination of annual demands. However, it is quite difficult to find an absolute critical

combination of annual demands. Rather an approximate critical combination can be found using an exhaustive search method in combination with a GA. The size of several approximate critical combinations of annual demands can be compared in order to find the optimal one for sizing a HRES.

The flow chart for finding an approximate critical combination of annual demands is shown in Fig. 4.2. The method starts by optimizing the size of a HRES for zero LPSP with a typical hourly average daily demand profile repeated throughout the year. The size can then be used with randomly generated annual demand profile to determine the LPSP. The newly generated annual demand profile that can not satisfy the desired zero LPSP by the system would be recorded. Subsequently the size of the lowest energy density source is increased in order to meet the desired LPSP for the recorded random demand profile.

This method was repeated as long as the new HRES could not satisfy any annual demand profile that was generated with random variations. The demand profile for which the change in size of a HRES had last been required, was considered as an approximate critical combination of annual demands. This approximate critical combination of annual demands was then used for optimal sizing of a HRES using a GA.

Repeating this method ended with multiple optimal size of a HRES for several approximate critical combinations of annual demands. If the sizes could satisfy any randomly varied demand profiles with the desired LPSP, then the system with lowest cost was considered to

be the optimal one. However, if none of the sizes could satisfy the desired LPSP for all the recorded randomly varied demand profiles the sizes could be compared in order to find an optimal one. The HRES which could satisfy all recorded demand profiles for the desired reliability and a minimum cost, was taken as the optimal size.

4.3.1 Results and Discussion

At the beginning of this investigation, the system was sized using a GA optimization method as shown in Fig. 2.7 for the average hourly load repeated throughout the year and the results are presented in Table 4.1.

Table 4.1 Optimal size of a HRES with typical annual demand

Method Name	WG #	PV #	Bat #	Height (m)	Tilt angle (°)	Total Cost (\$)
GA	6	81	18 (9 × 2)	29	53	303,644

Now, the load of Figure 4.1 is considered to vary randomly within a range of $\pm 25\%$ (in magnitude) of the values and temporal position in each group from 07:00 hr to 12:00 hr and from 16:00 hr to 21:00 hr. This is done to simulate the variation of user action and environmental effect. At the beginning of a GA optimization method, a time varying demand profile was generated and used for sizing a HRES. Several runs of the method resulted in different sizing optimization of the HRES due to the random variation of the peak demand. In all cases, LPSP was taken as the reliability index and the system was sized for zero LPSP. Table 4.2 shows optimal sizes of a HRES due to random demand variations from three runs

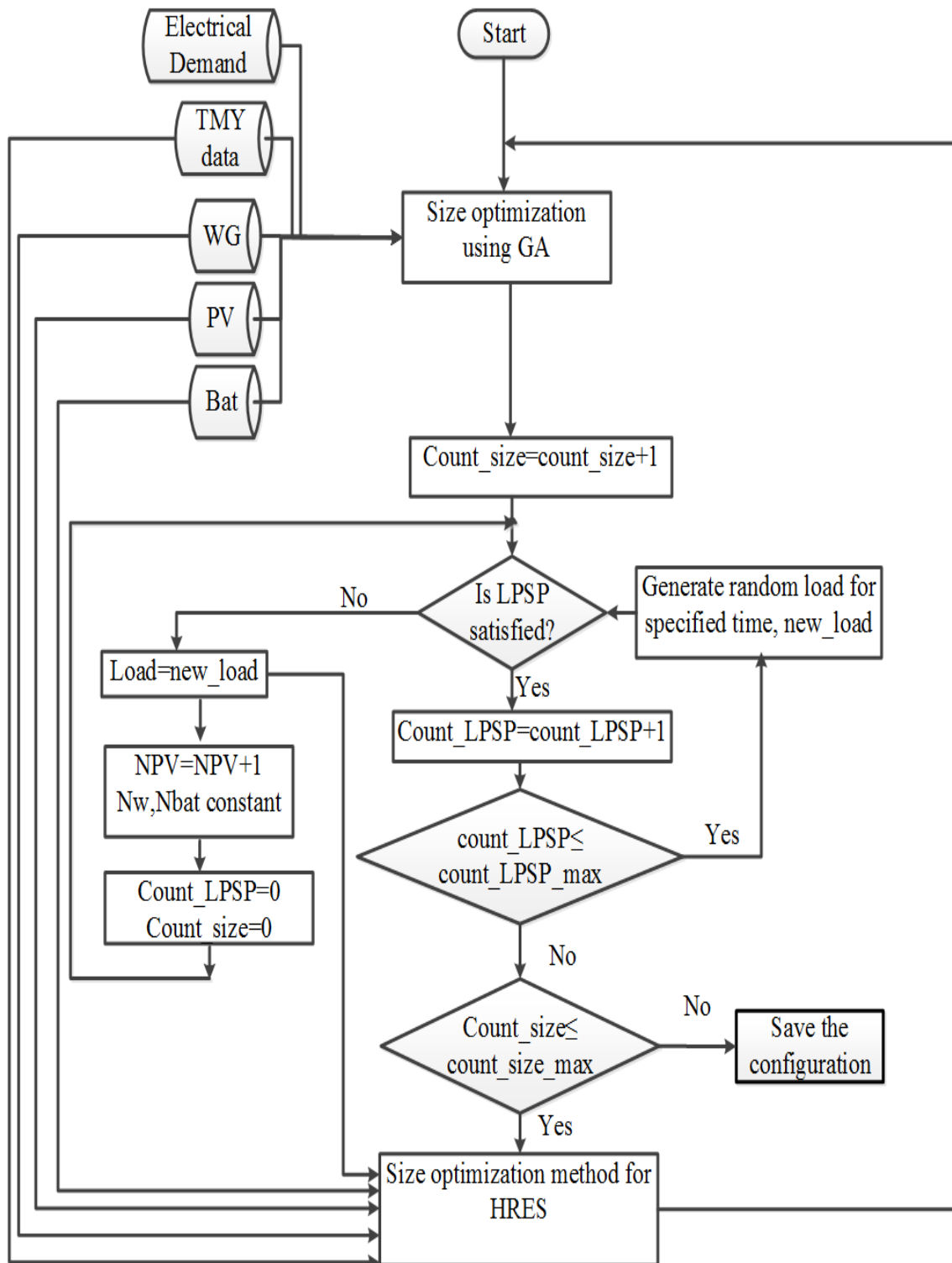


Fig. 4.2 Flow chart for generating approximate critical combination of annual demand profile.

of GA .

Table 4.2 Optimal size of a HRES from three run of GA with random load variations

Method Name	WG #	PV #	Bat #	Height (m)	Tilt angle (°)	Total Cost (\$)
GA	6	84	18 (9 × 2)	28	58	308,700
GA	9	77	14 (7 × 2)	29	43	288,385
GA	7	75	18 (9 × 2)	28	58	333,320

The results suggested that random variation of the peak demand in the annual profile affect the size of a HRES significantly. In the worst case size, the number of PV modules, WGs and batteries has changed from 81, 6, 16 to 75, 7, 18 and the WG installation height and PV module tilt angle were changed from 29m, 53° to 28m, 58° respectively. The optimized HRES was taken as having a total cost of \$333,320 as suggested in [70]. However, the system was unable to meet all demand profile generated by random variations. Thus, the system was sized using the method suggested in Fig. 4.2.

Several runs of the whole procedure resulted in several optimal sizes with different approximate critical hourly demand profile of a year as shown in Table 4.3.

None of the systems in Table 4.3 could satisfy all the recorded demand profiles (Appendix A) with the desired reliability. In all the system, the number of WG was 7 while the number of

Table 4.3 Optimal size of a HRES for typical and critical hourly load profile

WG #	PV #	Bat #	Height (m)	Tilt angle (°)	Total Cost (\$)
7	103	16 (8 × 2)	31	34	329,108
7	75	18 (9 × 2)	28	58	333,320

PV modules and batteries varies from 75 to 103 and from 16(8 × 2) to 18(9 × 2) respectively. Hence, the optimal system configurations were assumed to be within these ranges. Assuming the number of batteries is 16, the number of PV modules is changed using the bi-section [75] method and tested for all the recorded random hourly load profiles. The minimum number of PV modules that satisfied all loads was considered as one of the optimal sizes. This technique was subsequently repeated by increasing the number of batteries to 18. With this method, it was possible to record two probable systems for randomly varied demand profiles, as shown in Table 4.4.

Table 4.4 Probable optimal size of a HRES for hourly varied random load profile

WG #	PV #	Bat #	Height (m)	Tilt angle (°)	Total Cost (\$)
7	88	18 (9 × 2)	28	58	333,320
7	141	16 (8 × 2)	34	38	433,460

Both systems in Table 4.4 were tested for the randomly varied loads generated by the GA. If the systems were able to meet any randomly varied demands generated by the GA, the

system with the lowest cost was considered as the optimal system. This process resulted in the optimal size as shown in Table 4.5.

Table 4.5 Probable optimal size of a HRES for hourly varied random load profile

WG #	PV #	Bat #	Height (m)	Tilt angle (°)	Total Cost (\$)
7	88	18 (9 × 2)	28	58	343,305

Further, it was noticed that there was negligible change to the amount of total annual energy demand for a randomly varying load profile. The maximum and minimum electrical demand in the profile was the same for each demand profile as shown in Appendix A. However, it is shown in chapter 3 that the system optimized for an average of randomly varied demand profiles repeated throughout the year can not satisfy all time varying annual demand profile with the desired reliability. This is due to fact that the temporal position of peak demand varies with each load profile.

4.4 Concluding remarks

It is evident from the presented results that the optimal size of a HRES varies significantly when random variations of the load are considered, both in magnitude and temporal position. It is also to be understood that the hourly electrical demand of a day will not repeat throughout the year rather it would vary significantly due to both user action and seasonal variations. This finding is significant as random variation in the magnitude and time distribution of loads

is very common in real systems [70].

It is suggested in this chapter that the optimal sizing of a HRES needs to consider random variations both in magnitude and temporal position. Furthermore, a method for finding critical combination of annual demand profile is suggested and that profile is used for finding optimal size that can satisfy any randomly varied profiles. The method for finding a critical combination of annual demands with genetic algorithms can be incorporated with any other optimization for sizing a HRES with time varying demand profile.

Chapter 5

Optimal Size Integrating Demand Side Management

5.1 Introduction

As has already been noted, the optimal selection and sizing of distributed energy resources is crucial in order to deliver lowest investment cost and ensure adequate and full use of resources while the desired reliability is achieved. Different optimization methods have been suggested in this regard including linear programming (LP) [34], exhaustive search methods (iterative method) [22, 25–27, 29, 31], genetic algorithms (GA) [17, 18], particle swarm optimization (PSO) [76, 77], Markov chain model with GA to expedite the optimization method [73], combined GA and simplex [41]. In almost all the above mentioned methods, the total investment of the system was minimized while matching the demand with the renewable generation for a desired reliability index, LPSP. The monthly average daily load, monthly

total demand or hourly demand of a day repeated throughout the year was considered in most of the previous studies. The chronological representation of average daily electrical load is usually preferred over others. However, the peak electrical load of daily demand profiles is greatly influenced by seasonal weather variations as well as socio-demographic factors. As the temporal distribution of this peak electrical demand does not usually match with the generation of the sources used in stand-alone hybrid renewable energy system (HRES), the size and the cost are increased significantly to meet the time varying demand profile with the desired reliability. It was shown in Chapter 4 that for demand profiles of similar total annual demand, the size of a HRES varied due to changes in temporal position of peak or maximum demand. Hence, the size of the HRES is essentially determined by the peak demand at off peak generation hours of a year and the temporal position of the peak demand. Electrical demand that varies daily and seasonally and the demand is largely uncontrollable and interruptions are very costly [78], therefore, the installed capacity is designed to meet maximum (peak) demand. Thus, the utilization factor and efficiency of the renewable energy generation remain very low while meeting the desired reliability at the lowest cost.

Utility companies usually finance and implement demand-side management (DSM) in order to control the end user energy consumption and thus reduce the peak and base loads [79] and improve the efficiency and utilization factor. This is achieved with the introduction of conservation and energy efficiency programs, by replacing fuel with renewable sources and management of residential and commercial demand [80–83]. Both the energy consumption cut-off and shifting the consumption from peak time to off-peak periods are the chief aims

of residential load management [84]. It was found in [85] that there is a significant scope for the application of DSM when the utilization (defined as the ratio of electricity demand to generation) is relatively low (about 50%). Therefore, the DSM has recently attracted the attention of the system planners for its ability to modify the demand profile and thus can reduce the investment cost. The key objectives of any DSM program are as follows [86]:

1. Energy efficiency focused on implementation of building, lighting and/or appliance improvement,
2. Energy efficiency focused on behavioral change and/or improved information and
3. Peak demand reduction program.

DSM programs include the use of efficient utilities, cutting peak demand and shifting peak demand loads to off-peak times. The strongest restriction of DSM is to change the daily routine in order to achieve load shifting. However, in private households, DSM is often used to limit demand from storage water heaters and heat pumps [86].

As DSM can balance the fluctuating renewable generation with the time varying demand profile by reducing the peak, it has the potential to reduce the investment cost of a HRES and improve its utilization factor. However, despite numerous studies, none considers DSM or the utilization factor in sizing a HRES. As such, this chapter examines several DSM options integrated with the optimal sizing of a wind (WG)-photovoltaic (PV)-battery HRES.

5.2 Demand profile

To size the system, the hourly household demand was obtained from the average hourly summer and winter domestic demand of Auckland, houses given in [74] and from the number of houses [87] as shown Fig. 5.1. The summer demand profile is almost constant from 06:00 hr to 18:00 hr at about 1500 W while the usage reduces significantly at night from 22:00 hr to 04:00 hrs. The winter energy use increases significantly from 07:00 hr till midnight and the peak winter demand reaches approximately 2600 W.

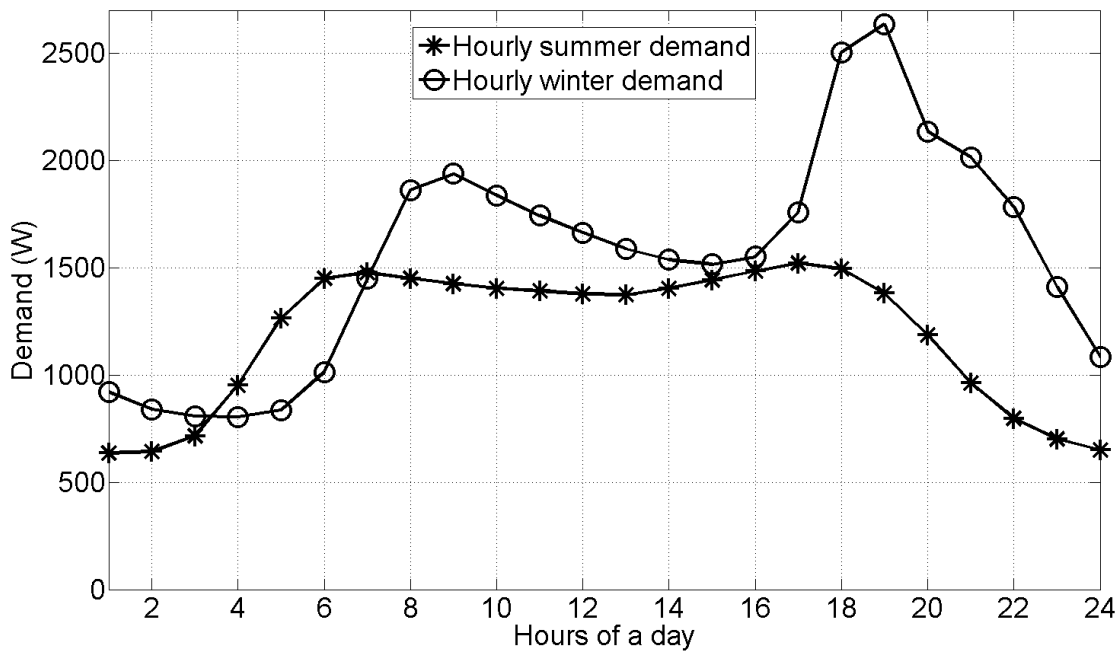


Fig. 5.1 Hourly winter and summer load of a day.

In order to generate an annual load profile, it was assumed that the winter profile could be applied between the month of April and October [88] while a summer load was applied for the remaining months.

As the input for the optimization, typical meteorological year (TMY) data for Auckland, New Zealand (latitude 36.85°S and longitude 174.78°E) was obtained from the U. S. Department of Energy [62].

5.3 DSM Options

The final component of the optimization was in the implementation of the DSM strategies. Previously it was noted that the annual seasonal demand profile was assumed to consist of a winter and summer portion. It was reported in [89] that approximately 45% of the total annual consumption of electricity was used for water and space heating in Auckland during the winter season. Hence it was decided that a DSM program should particularly target the additional winter demand and thus modify the shape of the electrical load profile. For this study, four options were examined:

Option-I Excess energy used for hot water and space heating,

Option-II Peak demand reduced throughout the year,

Option-III Peak demand reduced only while SOC reached a minimum and

Option-IV Fraction of peak load shifted to off peak hours.

5.4 Optimization Methodology

In order to determine the optimal size of the system a GA as shown in Fig. 2.7 was utilized. For the GA the number of chromosomes was taken to be 32, while each chromosome consisted of seven genes (variables) for investigating each DSM option and 8 for selecting a DSM option while sizing a HRES. They are $[N_{WG} N_{PV} N_{bat} h \beta ch f]$ where, $N_{PV} = (N_S \times N_P)$ is the number of photovoltaic modules, N_{WG} is the number of wind turbine generators, N_{bat} is the number of batteries, β is the PV tilt angle, h is the installation height of WG, ch is the choice of DSM program and f is the fraction of load curtailment and/or load shift.

5.5 Results and Discussion

5.5.1 Excess energy used for hot water and space heating

In Fig. 5.1 it was shown that energy consumption in winter is increased significantly from that of summer. As the first option for a DSM implementation, it was assumed that the additional energy consumption in winter was mainly due to water and space heating loads. Thus, the system was sized on the basis of a summer demand profile repeating throughout the year. During the winter months it was assumed that the additional electrical demand would be met from the excess energy generated by a system optimized for a summer only load profile, rather than having additional sources. In doing this there is an implicit assumption that the cost of using electricity hot water storage and heat storage is cheaper than the cost for the generation of electricity.

As such, a WG, PV and battery HRES were sized firstly for the hourly summer load repeated throughout the year and secondly for the hourly demand with seasonal variation. Table 5.1 shows the optimal size of the system for both the cases.

Table 5.1 Optimal size of the system for summer only and seasonal variations

Demand profile	WG #	PV #	Bat #	Height (m)	Tilt angle ($^{\circ}$)	Total Cost (\$)
Summer	5	70	14(7 × 2)	29	52	307,009
Winter-summer	5	100	18(9 × 2)	35	47	345,879

From Table 5.1, it can be seen that the size of the HRES increases significantly if the seasonal variations in annual load profile are considered. This is due to the fact that the total annual demand increases from 104,33 kWh to 122,83 kWh. At a supply level, the optimized size of a HRES using summer only demand generates approximately 239,91 kWh while a HRES system optimized for seasonal variations generates approximately 371,04 kWh. However it was noted that the increase in peak demand of the winter profile and its temporal position would require additional sources of generation to be met. This very high demand (greater than 2000 W) lasts only a few hours each day meaning that the additional sources which were utilized to meet this high demand would be generating significant excess energy outside this time. Thus, the utilization factor for the cases of demand profile consisting of seasonal variations was approximately 33% and 43% for a summer only load profile repeated throughout the year.

Now, Fig. 5.2 shows the variation in the state of the charge (SOC) of an optimal sized battery throughout the year. The state of charge of the battery reaches 0.22 at around 4200 hr and for a significant part of the year it is above 0.7. This indicates that the available energy from the renewable resources at 4200 hr was very low compared to the electrical load. Thus, the size of HRES was increased to cope with this demand and was the excess capacity for the remainder of the year.

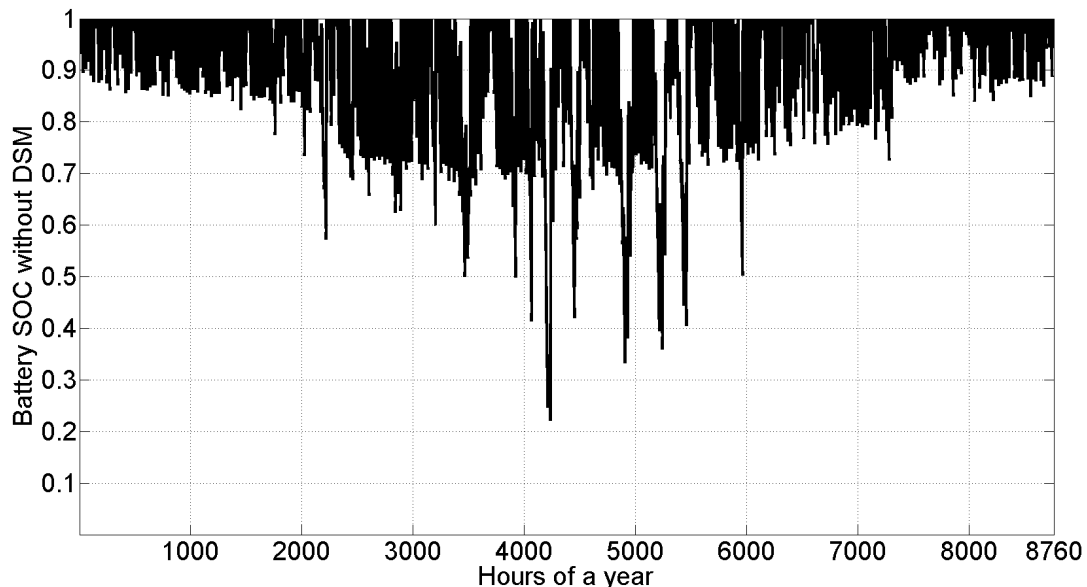


Fig. 5.2 The variation of the SOC throughout the year for summer only demand.

To explore this further, it was found that the average increase demand during the winter season was approximately 400 Wh while the average excess energy (additional to summer demand) generated by the system optimized considering a summer only load was around 700 Wh. In a typical HRES, this excess generation would be wasted through a dump load to ensure system stability and would require additional capital outlay, however it is possible to

instead utilize thermal storage as this “dump load”.

Illustrating this point, Fig. 5.3 and Fig. 5.4 show the increase in additional winter demand and excess energy generated by the system optimized considering summer only demand between 3500 hr to 4500 hr of a year. From these it can be concluded that the increase in additional winter energy demand could be satisfied by the excess generated energy from a “summer only” system. In doing so, the system utilization can be improved and the cost of the energy can be reduced significantly, as the utilization factor in the case of a system sized on the basis of summer only demand and used to meet the winter load, increases to 51%.

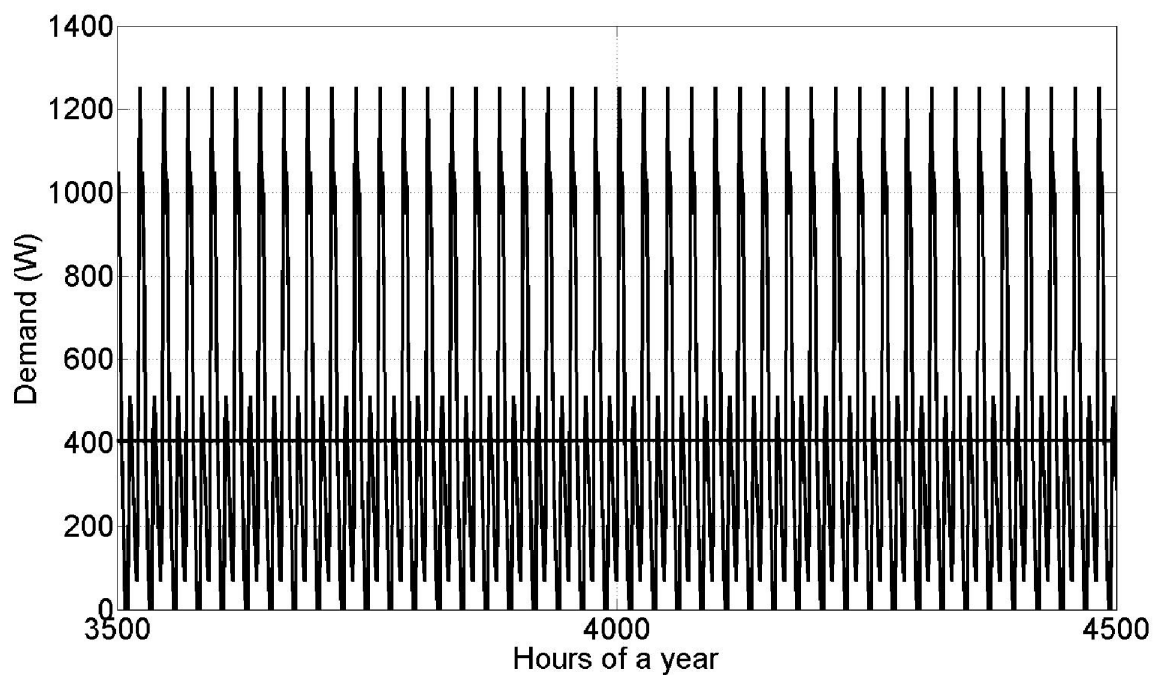


Fig. 5.3 The additional energy demand in winter session as compared to summer demand.

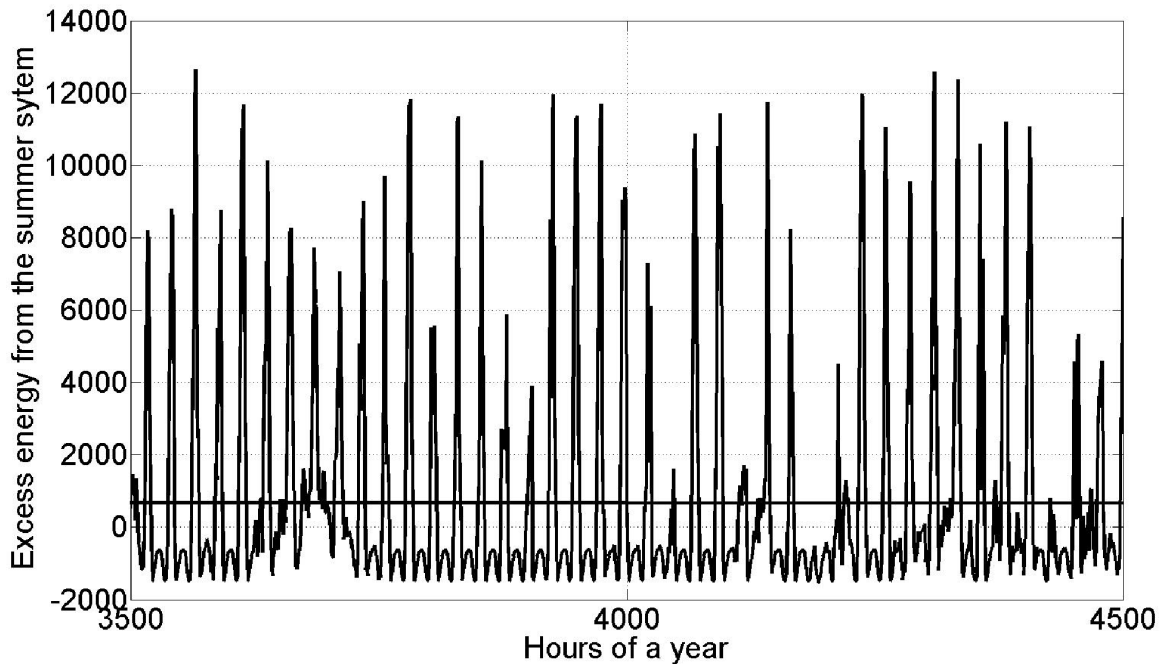


Fig. 5.4 The excess energy generation from the system optimized only for summer load.

5.5.2 Peak demand reduced throughout the year

The second option for DSM was to clip the peaks in the combined summer and winter demand profile. In doing this the size of the system was optimized with the aim of curtailing peak demand throughout the year. The curtailed electrical demand required an adjustment to the usage pattern of the electrical load.

Hence the GA was used to select the amount of curtailed load from the seasonal demand profile in addition to the size optimization of the HRES. Integrating this DSM option with the optimization method allowed the determination of an optimal load reduction rather than merely reducing the total excess winter demand to match a year of summer demand only. In doing this it was found that this would require a 40% reduction to the winter peak load.

Hence a modified winter load was developed and Fig. 5.5 illustrates this from 4140 hr to 4280 hr of the year.

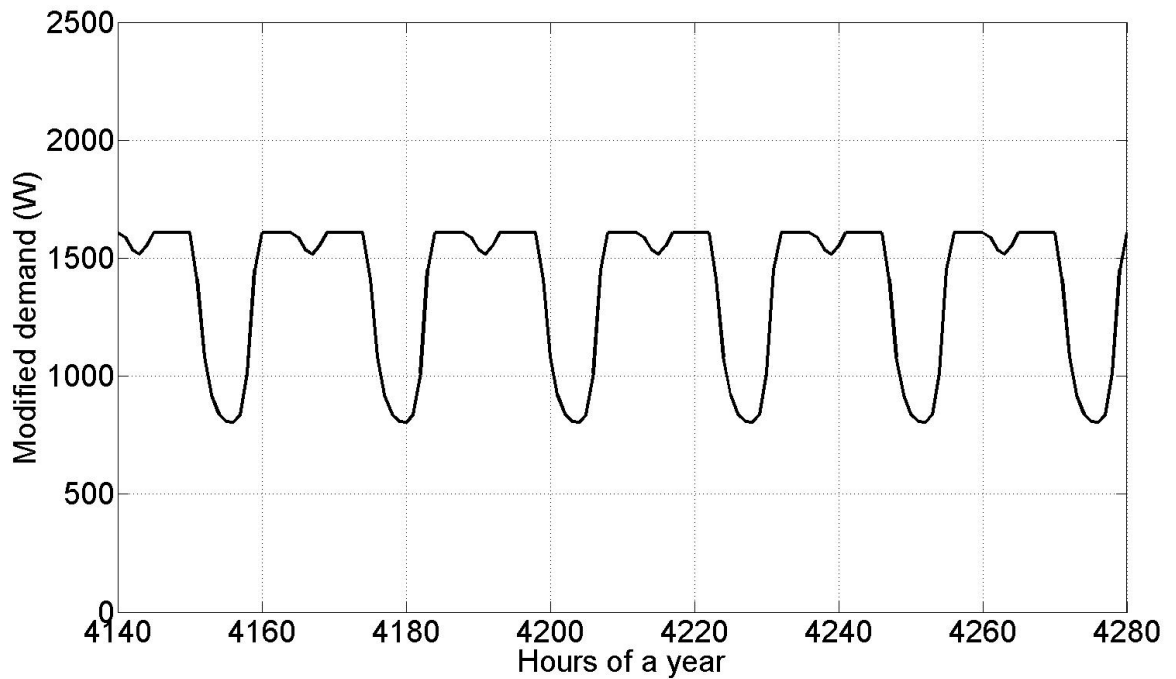


Fig. 5.5 The modified winter load from 4140 hrs to 4280 hr of a year.

The system cost for the curtailed load throughout the year is shown in Table 5.2. It is evident that the total system cost is slightly higher than the cost of summer only system. However, it is lower than that of the system for annual load profile consisted of hourly winter and summer load. The new load has a peak demand of 1607 W which is slightly higher than the summer peak demand.

As the load was curtailed with the same amount throughout the year the system cost was reduced and an optimized size was reached. In achieving this the utilization factor of the

optimized system is approximately 42%.

Table 5.2 Optimal size of a system for summer for curtailed load due to seasonal variation

Demand profile	WG #	PV #	Bat #	Height (m)	Tilt angle (°)	Curtailed energy (%)	Total Cost (\$)
Winter-Summer	9	75	16 (8 × 2)	20	53	39	310,928

5.5.3 Peak demand reduced when SOC is low

For the third DSM option, the demand profile consisted of a seasonally varying load (winter and summer load) and loads were clipped when the battery's state of charge was particularly low. The state of charge (SOC) of the optimal sized battery as shown in Fig. 5.2 revealed that it reached its lowest level during the period of minimum energy generation. Thus, this DSM option could be used to curtail the peak demand around the hours of a year where the SOC reaches a pre-set lower level, instead of reducing the load by the same level throughout the year. In doing this, both the lower level of the pre-set SOC and the amount of peak load which was to be clipped, were selected using the GA.

Now Fig. 5.2 showed the battery SOC before any DSM option was selected. From this it was seen that the SOC reached its minimum value during the hours from 4000 to 5500 of the year. Thus, this DSM option is aimed at curtailing the load only around the hours where the SOC is close to the pre-set level of SOC, this results in the modified load profile shown in

Fig. 5.6.

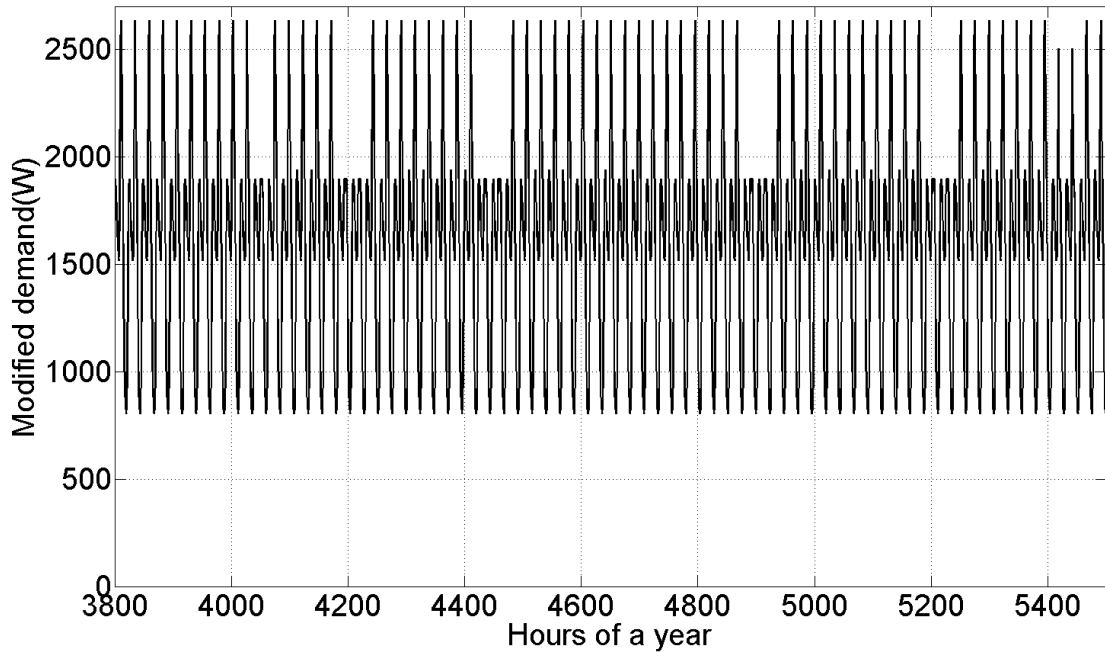


Fig. 5.6 Electrical load is modified as per minimum SOC.

The demand profile is modified only few times throughout the year rather than it is modified throughout the year. It is also explored that the load is reduced only the hours where the SOC reached below 0.4. The load is reduced approximately 1900 W from 2600 W. The load as modified by the optimization method from 4140 hr to 4280 hr of a year is shown in Fig. 5.7.

In Fig. 5.7 it can be seen that the peak load, as modified by the optimization method, is reduced from around 2600 W to 1900 W from 4180 hr to 4230 hr. As such, the optimized system size and the amount of curtailed load and the set minimum SOC are shown in Table 5.3.

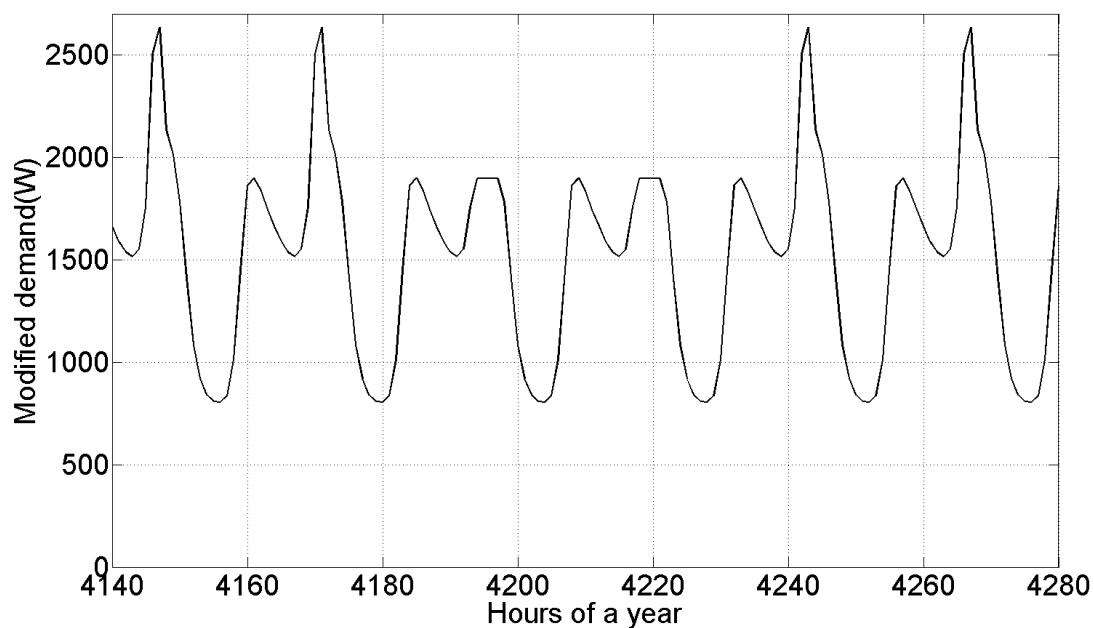


Fig. 5.7 Modified load from hours 4140 to 4280 of a year.

Table 5.3 Optimal size of a system for modified demand as per minimum SOC

Demand profile	WG #	PV #	Bat #	Height (m)	Tilt angle (°)	Curtailed energy (%)	Total Cost (\$)
Winter-Summer	9	108	16 (8 × 2)	13	31	28	333,626

In Fig. 5.8 it is clearly evident that the SOC has been updated with the modified load. It can be seen that the SOC of the optimized size battery reaches 0.7 or lower more frequently than that without any DSM option.

The utilization factor for the system was reduced to 33% which was 36% percent in case of

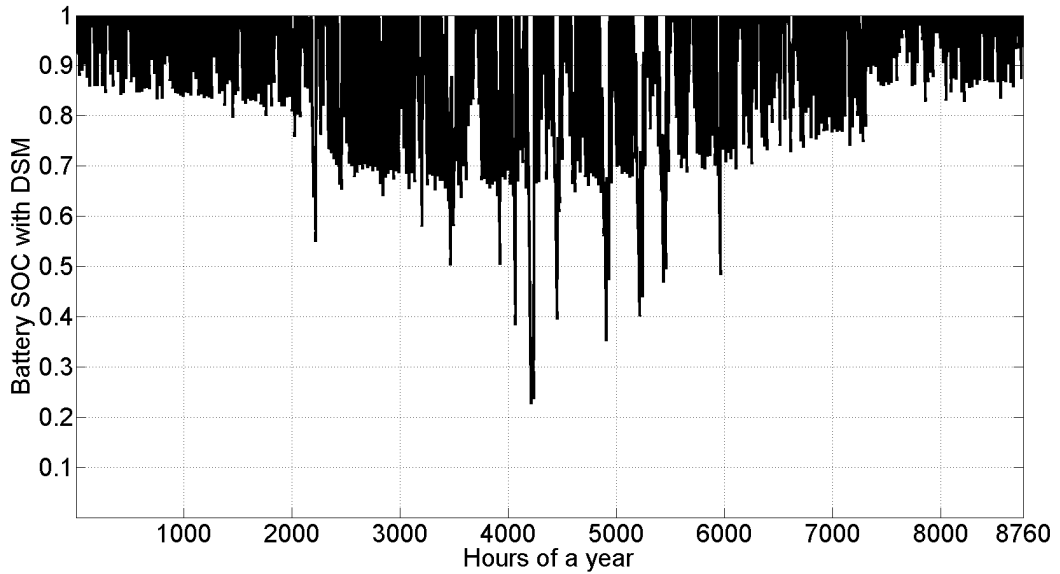


Fig. 5.8 The variation of the SOC throughout the year due to modified new load as per minimum SOC

the system optimized for the annual load consisted of winter and summer seasonal loads.

5.5.4 Fraction of peak load shifted to off peak hours

The final DSM strategy aimed to smooth the load profile through a load shifting strategy implemented on a seasonally varying demand profile. It is clear that the peak of the hourly winter load can dictate the size of a HRES when an annual load with seasonal variations is considered. Thus, this DSM program would reduce the loading from 08:00 hr to 22:00 hr and shift this to 01:00 hr to 06:00 hr. In doing this the amount of curtailed and shifted load would be determined by the GA. As such the modified winter demand of a typical day is shown in Fig. 5.9.

The winter peak demand from 07:00 hr to 24:00 hr is reduced and the off-peak demand during 01:00 hr to 06:00 hr is increased. The DSM option is used to reduce the peak demand and some fraction of this demand is shifted to the off peak period. The option has not meant to shift the total amount of curtailed demand to the off peak period, rather the method is used to find the optimal amount of curtailed and shifted peak demand. The modified winter demand of a day is shown in Fig. 5.9.

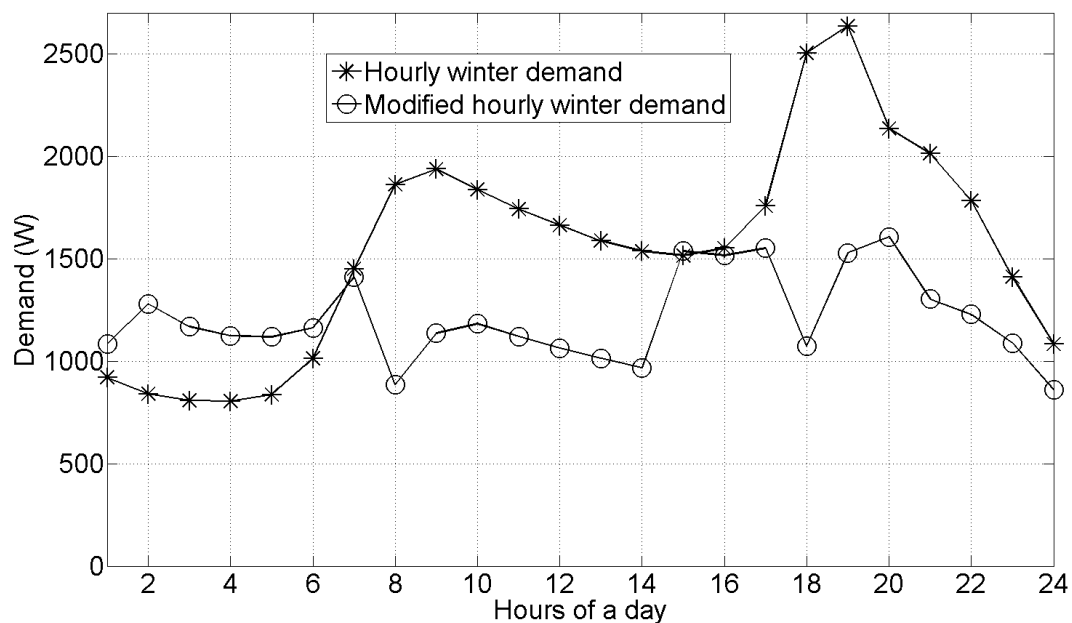


Fig. 5.9 Modified demand shift as fraction of winter load shifted from peak to off-peak hours.

With this modification to the winter demand throughout the year, the optimal sizing has seen a reduction of the storage size significantly from 18 to 14 batteries as shown in Table 5.4. However in achieving this the utilization factor of the system is reduced, but, there is a significant saving in the total investment cost.

Table 5.4 Optimal size of a system with reduced and shift of peak demand

Demand profile	WG #	PV #	Bat #	Height (m)	Tilt angle (°)	Curtailed energy (%)	Total Cost (\$)
Winter-Summer	5	100	14 (7 × 2)	13	27	40	286,297

The modified profile shows almost an equal temporal distribution of electrical demand. The peak demand is reduced to approximately 1600 W. The total system cost has reduced to \$286,297 which is lowest among all the options. However, the utilization factor is also reduced to 28.05% .

5.6 Concluding remarks

In this study it was found that the investment cost of a HRES due to time varying electrical demand usually increased significantly and the size of a HRES is usually dictated by the temporal position of peak electrical demand as well as total electrical demand. It was found in this study that integrating DSM with optimal sizing method could reduce total investment cost. Among the various DSM options, the system cost is reduced when sizing a system considering summer load throughout the year and the increased winter demand is met from the excess energy generated by the system. Further, the utilization factor of generated energy from the designed system is increased to maximum.

It is further noted that the system size could be reduced without modifying the demand throughout the year but rather limiting the electrical usage for only a few hours of the year.

However, among the four different choices, Option IV provides the lowest total system cost but the system has a low utilization factor. Furthermore, there is a probability that the curtailed energy would affect the life of consumers. However, the GA would always suggest option IV due to the low total system cost.

Chapter 6

Conclusion and Future Work

The stochastic nature of renewable energy generation and demand profile, and non-linear system characteristics make the optimal sizing of a HRES much more complex and difficult. The application of an optimization method is thus required to match the renewable energy generation to the demand profile. This requires both utilization of efficient optimization methods and representation of real life demand profiles. In this study, different aspects of demand profiles and their effects on optimal sizing of a HRES were investigated. The magnitude and temporal position of peak hourly demand vary due to different factors such as socio-demographic, socio-economic and seasonal variations. It was also found that randomness of the demand profile which is common in real life, and was ignored in previous studies, significantly influenced the optimal size of a HRES. It was also noticed that the optimal system for a typical fixed hourly load of day repeated throughout the year was not able to meet the desired reliability due to stochastic variation both in magnitude and temporal position of peak hourly demand in the annual demand profile. It was further observed that the

size of a HRES depends not only on the total annual electrical load but also on the magnitude and temporal position combination of peak demand in an annual profile. The size of a HRES considering a fixed average demand profile repeated throughout the year was unable to meet the desired reliability due to the randomness of the load. The optimized size of a HRES due to randomly varied demand profile is increased significantly compared to a fixed typical daily demand profile.

The magnitude and temporal position of peak energy demand are greatly influenced by the socio-demographic factors and seasonal weather variation. In this case, monthly average daily profiles had been considered during the analysis. Thus, impact of seasonal variation was also incorporated with that analysis. Socio-demographic demand profiles were used to examine the effect of the temporal position and magnitude of peak demand in a daily profile on the optimal size of a HRES. It was shown that the optimal sized HRES for a site would meet the demand profiles with minimum LPSP, thus included socio-demographic factors.

Demand side management (DSM) was incorporated for its ability to modify the demand profile and reduce the size of a system as well as improve utilization factors. The investigation suggested that the investment cost could be reduced with the integration of DSM in optimal sizing of a HRES. This reduced cost would be an incentive for an investor to make a choice. However, due to the lack of appliance specific demand data it was not possible to determine the affect of DSM on the consumer. In this respect there are a number of avenues of research that may be pursued in the future.

1. In this research work, monthly average daily demand data of 40 houses was considered in order to find link of socio-demographic factors on optimal size of a HRES. Although, 239 demand profiles are enough to infer the influence of socio-demographic factors on optimal size of a HRES, a large number of demand profiles and more information regarding consumers such as financial status, use of appliances and age, would enable a better understanding of what socio-demographic factors determine the profile class. Additionally, the classification of demand profiles would be more representative to their classes if a large number of demand profiles were used.
2. Optimal sizing of a HRES requires real life load profiles rather than typical ones. The modeling of real life demand profiles is a challenging task. Artificial intelligence techniques have been investigated for modeling or forecasting residential demand profiles, these could be incorporated with the optimal sizing and control of a HRES.
3. Innovative control methods and DSM could play a major role in reducing the investment cost while sizing a HRES. Curtailing or shifting the electrical demand for short time intervals over a year, where the renewable generation is very low, may reduce the size of the system. The residential demand profile required could be investigated further in this regard.
4. More robust optimization techniques should be investigated and applied so that computation time can be reduced and convergence to sub-optimal solutions can be avoided.

5. Finally, a small pilot project could be initiated and investigated for future studies including DSM.

References

- [1] M. R. Patel, *Wind and Solar Power Systems: Design, Analysis and Operation*. Washington, USA: CRC press, 2005.
- [2] E. Papadopoulou, *Photovoltaic Industrial Systems: An Environmental Approach*. Berlin, Heidelberg: Springer-Verlag, 2011.
- [3] W. Zhou, “*Simulation and Optimum Design of Hybrid Solar-Wind and Solar-Wind-Diesel Power Generation Systems*,” Ph.D. dissertation, The Hong Kong Polytechnic University, Hong Kong, 2008.
- [4] U. S. Department of State, “Projected Greenhouse Gas Emission,” in *United States Climate Action Report*. U. S. Department of State, Washington, USA, 2014, pp. 134–150.
- [5] Global Wind Energy Council, “*Global Wind Report-Annual Market Update 2013*.” Global Wind Energy Council, Belgium, 2013.
- [6] W. E. Glassley, *Geothermal Energy: Renewable Energy and the Environment*, 2nd ed. New York: CRC Press, 2014.

- [7] E. Barbier, “Geothermal Energy Technology and Current Status: An Overview,” *Renewable and Sustainable Energy Reviews*, vol. 6, no. 1, pp. 3–65, 2002.
- [8] “Geothermal Energy and Electricity Generation,” http://www.nzgeothermal.org.nz/elec_geo.html, accessed: October 12, 2015.
- [9] Y. D. Goswami, F. Kreith, and J. F. Kreider, *Principles of Solar Engineering*. Washington, USA: Hemisphere Publishing Corporation, 1978.
- [10] T. Markvart, *Solar Electricity*, 2nd ed. West Sussex, England: John Wiley & Sons Ltd, 2000.
- [11] F. Trieb, C. Schillings, M. O’Sullivan, T. Pregger, and C. Hoyer-Klick, “Global Potential of Concentrating Solar Power,” in *SolarPaces Conference Proceedings*, Berlin, Germany, 15-18 September, 2009.
- [12] International Renewable Energy Agency, “*Renewable Energy Costs, Technologies and Markets*,” <http://costing.irena.org/charts/solar-photovoltaic.aspx>, accessed: June 02, 2015.
- [13] Global Wind Energy Council, “*Global Wind Report-Annual Market Update 2014*.” Global Wind Energy Council, Belgium, 2014.
- [14] G. Kelly, “History and Potential of Renewable Energy Development in New Zealand,” *Renewable and Sustainable Energy Reviews*, vol. 15, no. 5, pp. 2501–2509, 2011.
- [15] O. Paish, “Small Hydro Power: Technology and Current Status,” *Renewable and Sustainable Energy Reviews*, vol. 6, no. 6, pp. 537–556, 2002.

- [16] Ministry for the Environment, “Environmental Report Card.” Wellington: Ministry for the Environment, July, 2009.
- [17] H. Yang, W. Zhou, L. Lu, and Z. Fang, “Optimal Sizing Method for Stand-Alone Hybrid Solar-Wind System with LPSP Technology by Using Genetic Algorithm,” *Solar Energy*, vol. 82, no. 4, pp. 354–367, 2008.
- [18] E. Koutroulis, D. Kolokotsa, A. Potirakis, and K. Kalaitzakis, “Methodology for Optimal Sizing of Stand-Alone Photovoltaic/Wind-generator Systems Using Genetic Algorithms,” *Solar Energy*, vol. 80, no. 9, pp. 1072–1088, 2006.
- [19] M. Deshmukh and S. Deshmukh, “Modeling of Hybrid Renewable Energy Systems,” *Renewable and Sustainable Energy Reviews*, vol. 12, no. 1, pp. 235–249, 2008.
- [20] H. Chen, T. N. Cong, W. Yang, C. Tan, Y. Li, and Y. Ding, “Progress in Electrical Energy Storage System: A Critical Review,” *Progress in Natural Science*, vol. 19, no. 3, pp. 291–312, 2009.
- [21] M. A. Bhatti, *Practical Optimization Methods: with Mathematica Applications*. New York, USA: Springer-Verlag New York, Inc., 2000.
- [22] B. S. Borowy and Z. M. Salameh, “Methodology for Optimally Sizing the Combination of a Battery Bank and PV Array in a Wind/PV Hybrid System,” *IEEE Transactions on Energy Conversion*, vol. 11, no. 2, pp. 367–375, 1996.
- [23] T. Markvart, “Sizing of Hybrid Photovoltaic-Wind energy Systems,” *Solar Energy*, vol. 57, no. 4, pp. 277–281, 1996.

- [24] W. Zhou, C. Lou, Z. Li, L. Lu, and H. Yang, "Current Status of Research on Optimum Sizing of Stand-Alone Hybrid Solar-Wind Power Generation Systems," *Applied Energy*, vol. 87, no. 2, pp. 380–389, 2010.
- [25] B. S. Borowy and Z. M. Salameh, "Optimum Photovoltaic Array Size for a Hybrid Wind/PV System," *IEEE Transactions on Energy Conversion*, vol. 9, no. 3, pp. 482–488, 1994.
- [26] B. Ai, H. Yang, H. Shen, and X. Liao, "Computer-Aided Design of PV/Wind Hybrid System," *Renewable Energy*, vol. 28, no. 10, pp. 1491–1512, 2003.
- [27] W. Kellogg, M. Nehrir, G. Venkataramanan, and V. Gerez, "Generation Unit Sizing and Cost Analysis for Stand-Alone Wind, Photovoltaic and Hybrid Wind/PV Systems," *IEEE Transactions on Energy Conversion*, vol. 13, no. 1, pp. 70–75, 1998.
- [28] S. Ashok, "Optimised Model for Community-Based Hybrid Energy System," *Renewable Energy*, vol. 32, no. 7, pp. 1155–1164, 2007.
- [29] S. Diaf, M. Belhamel, M. Haddadi, and A. Louche, "Technical and Economic Assessment of Hybrid Photovoltaic/Wind System With Battery Storage in Corsica Island," *Energy Policy*, vol. 36, no. 2, pp. 743–754, 2008.
- [30] A. Kaabeche, M. Belhamel, and R. Ibtouen, "Sizing Optimization of Grid-Independent Hybrid Photovoltaic/Wind Power Generation System," *Energy*, vol. 36, no. 2, pp. 1214–1222, 2011.

- [31] H. Yang, L. Lu, and W. Zhou, "A Novel Optimization Sizing Model for Hybrid Solar-Wind Power Generation System," *Solar Energy*, vol. 81, no. 1, pp. 76–84, 2007.
- [32] S. Paudel, J. N. Shrestha, F. J. Neto, J. A. Ferreira, and M. Adhikari, "Optimization of Hybrid PV/Wind Power System for Remote Telecom Station," in *IEEE International Conference on Power and Energy Systems (ICPS)*, Chennai, 22-24 Dec., 2011, pp. 1–6.
- [33] A. De and L. Musgrove, "The Optimization of Hybrid Energy Conversion Systems Using the Dynamic Programming Model—RAPSODY," *International Journal of Energy Research*, vol. 12, no. 3, pp. 447–457, 1988.
- [34] R. Chedid and S. Rahman, "Unit Sizing and Control of Hybrid Wind-Solar Power Systems," *IEEE Transactions on Energy Conversion*, vol. 12, no. 1, pp. 79–85, 1997.
- [35] D. Xu, L. Kang, L. Chang, and B. Cao, "Optimal Sizing of Standalone Hybrid Wind/PV Power Systems Using Genetic Algorithms," in *IEEE Canadian Conference on Electrical and Computer Engineering*, Saskatoon, 01-04 May, 2005, pp. 1722–1725.
- [36] A. Shahirinia, S. Tafreshi, A. H. Gastaj, and A. Moghaddomjoo, "Optimal Sizing of Hybrid Power System Using Genetic Algorithm," in *IEEE International Conference on Future Power Systems*, Amsterdam, 2005, pp. 1–6.
- [37] R. Gupta, R. Kumar, and A. K. Bansal, "Economic Analysis and Design of Stand-Alone Wind/Photovoltaic Hybrid Energy System Using Genetic Algorithm," in *IEEE*

- International Conference on Computing, Communication and Applications (ICCCA)*, Dindigul, Tamilnadu, 22-24 Feb., 2012, pp. 1–6.
- [38] S. Hakimi, S. M. Tafreshi, and A. Kashefi, “Unit Sizing of a Stand-Alone Hybrid Power System Using Particle Swarm Optimization (pso),” in *IEEE International Conference on Automation and Logistics*, Jinan, 18-21 Aug. 2007, pp. 3107–3112.
- [39] A. K. Kaviani, G. Riahy, and S. M. Kouhsari, “Optimal Design of a Reliable Hydrogen-Based Stand-Alone Wind/PV Generating System, Considering Component Outages,” *Renewable Energy*, vol. 34, no. 11, pp. 2380–2390, 2009.
- [40] F. Jahanbani and G. H. Riahy, “Optimum Design of a Hybrid Renewable Energy System,” in *Renewable Energy -Trends and Applications*. INTECH Open Access Publisher, 2011, pp. 231–250.
- [41] J. Lagorse, D. Paire, and A. Miraoui, “Sizing Optimization of a Stand-Alone Street Lighting System Powered by a Hybrid System Using Fuel Cell, PV and Battery,” *Renewable Energy*, vol. 34, no. 3, pp. 683–691, 2009.
- [42] F. McLoughlin, A. Duffy, and M. F. Conlon, “The Generation of Domestic Electricity Load Profiles Through Markov Chain Modelling,” *Euro-Asian Journal of Sustainable Energy Development Policy*, vol. 3, 2010.
- [43] I. Knight and H. Ribberink, *European and Canadian Non-HVAC Electric and DHW Load Profiles for Use in Simulating the Performance of Residential Cogeneration*

- Systems*. International Energy Agency, Annex 42-FC+COGEN+SIM, Subtask A, May, 2007.
- [44] I. Mansouri, M. Newborough, and D. Probert, “Energy Consumption in UK Households: Impact of Domestic Electrical Appliances,” *Applied Energy*, vol. 54, no. 3, pp. 211–285, 1996.
- [45] S. Firth, K. Lomas, A. Wright, and R. Wall, “Identifying Trends in the Use of Domestic Appliances from Household Electricity Consumption Measurements,” *Energy and Buildings*, vol. 40, no. 5, pp. 926–936, 2008.
- [46] G. Wood and M. Newborough, “Dynamic Energy-Consumption Indicators for Domestic Appliances: Environment, Behaviour and Design,” *Energy and Buildings*, vol. 35, no. 8, pp. 821–841, 2003.
- [47] H. Chen, C. A. Canizares, and A. Singh, “ANN-Based Short-Term Load Forecasting in Electricity Markets,” in *IEEE Power Engineering Society Winter Meeting*, vol. 2, Columbus, OH, 28 Jan.-01 Feb., 2001, pp. 411–415.
- [48] University of Strathclyde Energy Systems Research Unit, “*Demand Profile Generators*,” http://www.esru.strath.ac.uk/EandE/Web_sites/06-07/Carbon_neutral/tools%20folder/Demand%20Profile%20Generators.htm, accessed: July 26, 2015.
- [49] M. Huamani and A. Orlando, “Methodology for Generating Thermal and Electric Load Profiles for Designing a Cogeneration System,” *Energy and Buildings*, vol. 39, no. 9, pp. 1003–1010, 2007.

- [50] R. Yao and K. Steemers, "A Method of Formulating Energy Load Profile for Domestic Buildings in the UK," *Energy and Buildings*, vol. 37, no. 6, pp. 663–671, 2005.
- [51] I. Baniasad Askari, L. Baniasad Askari, M. Kaykhah, and H. Baniasad Askari, "Optimisation and Techno-Economic Feasibility Analysis of Hybrid (Photovoltaic/Wind/Fuel Cell) Energy Systems in Kerman, Iran; considering the effects of electrical load and energy storage technology," *International Journal of Sustainable Energy*, vol. 33, no. 3, pp. 635–649, 2014.
- [52] A. Celik, "Optimisation and Techno-Economic Analysis of Autonomous Photovoltaic–Wind Hybrid Energy Systems in Comparison to Single Photovoltaic and Wind Systems," *Energy Conversion and Management*, vol. 43, no. 18, pp. 2453–2468, 2002.
- [53] S. Aissou, D. Rekioua, N. Mezzai, T. Rekioua, and S. Bacha, "Modeling and Control of Hybrid Photovoltaic Wind Power System with Battery Storage," *Energy Conversion and Management*, vol. 89, pp. 615–625, 2015.
- [54] D. Nelson, M. Nehrir, and C. Wang, "Unit Sizing and Cost Analysis of Stand-Alone Hybrid Wind/PV/Fuel Cell Power Generation Systems," *Renewable Energy*, vol. 31, no. 10, pp. 1641–1656, 2006.
- [55] T. Senjyu, D. Hayashi, A. Yona, N. Urasaki, and T. Funabashi, "Optimal Configuration of Power Generating Systems in Isolated Island with Renewable Energy," *Renewable Energy*, vol. 32, no. 11, pp. 1917–1933, 2007.

- [56] R. Billinton, R. N. Allan, and R. N. Allan, *Reliability Evaluation of Power Systems*. USA: Plenum Press New York, 1984, vol. 2.
- [57] R. Dufo-Lopez and J. L. Bernal-Agustín, “Design and Control Strategies of PV-Diesel Systems Using Genetic Algorithms,” *Solar Energy*, vol. 79, no. 1, pp. 33–46, 2005.
- [58] S. Hakimi, S. M. M. Tafreshi, and M. Rajati, “Unit Sizing of a Stand-Alone Hybrid Power System Using Model-Free Optimization,” in *IEEE International Conference on Granular Computing*, Fremont, CA, 2-4 Nov., 2007, pp. 751–751.
- [59] G. La Terra, G. Salvina, and G. Tina, “Optimal Sizing Procedure for Hybrid Solar Wind Power Systems by Fuzzy Logic,” in *IEEE Mediterranean Electrotechnical Conference*, Malaga, 16-19 May, 2006, pp. 865–868.
- [60] G. Tina, S. Gagliano, and S. Raiti, “Hybrid Solar/Wind Power System Probabilistic Modelling for Long-Term Performance Assessment,” *Solar Energy*, vol. 80, no. 5, pp. 578–588, 2006.
- [61] A. Stoecklein, A. Pollard, M. Camilery, J. Tries, and N. Isaacs, *The Household Energy End-Use Project: Measurement Approach and Sample Application of the New Zealand Household Energy Model*. Porirua, New Zealand: BRANZ, 2001.
- [62] US Department of Energy, “Weather data,” <http://apps1.eere.energy.gov/buildings/energyplus/weatherdata.about>, accessed January 30, 2013.
- [63] M. R. Patel, *Wind and Solar Power System*. Washington, USA: CRC Press, 1999.
- [64] P. Gipe, *Wind Energy Comes of Age*. John Wiley & Sons, New York, 1995.

- [65] J. A. Duffie and W. A. Beckman, *Solar Engineering of Thermal Processes*, 4th ed. John Wiley & Sons, Inc. New York, 2013.
- [66] D. Erbs, S. Klein, and J. Duffie, “Estimation of the Diffuse Radiation Fraction for Hourly, Daily and Monthly-Average Global Radiation,” *Solar Energy*, vol. 28, no. 4, pp. 293–302, 1982.
- [67] J. Orgill and K. Hollands, “Correlation Equation for Hourly Diffuse Radiation on a Horizontal Surface,” *Solar Energy*, vol. 19, no. 4, pp. 357–359, 1977.
- [68] D. T. Reindl, W. A. Beckman, and J. A. Duffie, “Diffuse Fraction Correlations,” *Solar Energy*, vol. 45, no. 1, pp. 1–7, 1990.
- [69] D. Guasch and S. Silvestre, “Dynamic Battery Model for Photovoltaic Applications,” *Progress in Photovoltaics: Research and Applications*, vol. 11, no. 3, pp. 193–206, 2003.
- [70] M. R. Tito, T. T. Lie, and T. Anderson, “Sizing Optimization of Wind-Photovoltaic Hybrid Energy Systems Under Transient Load,” *International Journal of Power and Energy Systems*, vol. 33, no. 4, pp. 168–174, 2013.
- [71] T. Kohonen, *Self-Organization and Associative Memory*, 3rd ed. New York: Springer-Verlag, 1989.
- [72] J. Widén, M. Lundh, I. Vassileva, E. Dahlquist, K. Ellegård, and E. Wäckelgård, “Constructing Load Profiles for Household Electricity and Hot Water from Time-Use

- Data—Modelling Approach and Validation,” *Energy and Buildings*,, vol. 41, no. 7, pp. 753–768, 2009.
- [73] Y.-Y. Hong and R.-C. Lian, “Optimal Sizing of Hybrid Wind/PV/Diesel Generation in a Stand-Alone Power System Using Markov-Based Genetic Algorithm,” *IEEE Transactions on Power Delivery*, vol. 27, no. 2, pp. 640–647, 2012.
- [74] S. K. Merz, “Auckland’s Electrical Demand Characteristics and Applicability of Demand Management.” Auckland, New Zealand: Sinclair Knight Merz, June, 2005.
- [75] D. Levy, “*Introduction to Numerical Analysis.*” USA: Department of Mathematics and Center for Scientific Computation and Mathematical Modeling, CSCAMM, University of Maryland, 2010.
- [76] A.-m. H. Hameed, M. T. Elhagri, A. Shaltout, M. M. A. Aziz *et al.*, “Optimum Sizing of Hybrid WT/PV Systems via Open-Space Particle Swarm Optimization,” in *IEEE Second Iranian Conference on Renewable Energy and Distributed Generation (ICREDG)*, Tehran, Iran, 6-8 March,2012, pp. 55–60.
- [77] M. Sharafi and T. Y. ELMekkawy, “Multi-Objective Optimal Design of Hybrid Renewable Energy Systems Using PSO-Simulation Based Approach,” *Renewable Energy*,, vol. 68, pp. 67–79, 2014.
- [78] G. Strbac, “Demand Side Management: Benefits and Challenges,” *Energy Policy*,, vol. 36, no. 12, pp. 4419–4426, 2008.

- [79] M. Ibrahim, M. Z. Jaafar, and M. Ab Ghani, "Demand-Side Management," in *IEEE Region 10 Conference on Proceedings. Computer, Communication, Control and Power Engineering*, vol. 4. Beijing, China: IEEE, 19-21 Oct., 1993, pp. 572–576.
- [80] B. Ramanathan and V. Vittal, "A Framework for Evaluation of Advanced Direct Load Control with Minimum Disruption," *IEEE Transactions on Power Systems*, vol. 23, no. 4, pp. 1681–1688, 2008.
- [81] C. W. Gellings and J. H. Chamberlin, "*Demand-Side Management: Concepts and Methods.*" The Fairmont Press Inc., Lilburn, GA, 1987.
- [82] M. A. A. Pedrasa, T. D. Spooner, and I. F. MacGill, "Scheduling of Demand Side Resources Using Binary Particle Swarm Optimization," *IEEE Transactions on Power Systems*, vol. 24, no. 3, pp. 1173–1181, 2009.
- [83] G. Brandon and A. Lewis, "Reducing Household Energy Consumption: A Qualitative and Quantitative Field Study," *Journal of Environmental Psychology*, vol. 19, no. 1, pp. 75–85, 1999.
- [84] A. Ipakchi and F. Albuyeh, "Grid of the Future," *IEEE Power and Energy Magazine*, vol. 7, no. 2, pp. 52–62, 2009.
- [85] KEMA Limited, "*Demand Side Management in Ireland-Evaluating the Energy Efficiency Opportunities.*" Sustainable Energy Ireland, Dublin, Ireland, January, 2008.

-
- [86] S. Funke and M. Speckmann, “Demand Side Management in Private Households—Actual Potential, Future Potential, Restrictions,” in *Energy-Efficient Computing and Networking*, Springer, 2011, pp. 29–36.
- [87] Auckland Regional Council, “*Housing and Households in the Auckland Region: Results from the 2006 Census of Population and Dwellings.*” Auckland: Auckland Regional Council, 2007.
- [88] T. N. Anderson, M. Duke, and J. K. Carson, “Performance of a Building Integrated Solar Combisystem,” in *Proceedings of 44th Annual Conference of the Australian and NZ Architectural Science Association*, Auckland, New Zealand, 2010.
- [89] N. P. Isaacs, *Supply Requires Demand: Where Does All of New Zealand’s Energy Go?* BRANZ, 2004.

Appendix A

A.1 Investigation on Time Varying load

The generated different random load profiles as generated and recorded in finding the approximate critical combination of annual demand profile was further investigated. The critical hourly demand of several days is shown in Fig. A.1. It is to be noted that there are day to day variations in the critical hourly demand profile of a year. This is more practical than the hourly load repeated throughout the year. It is more probable that the user will not repeat his or her action exactly at same hours of the day like a robot. This depends both on his or her availability and weather condition. Thus, it is expected that there will be variations of temporal location and amount of demand for a day.

The size of the system was varied significantly from the system as resulted by several runs of a GA. The PV modules were changed from 75 to 88 in numbers.

The generated different random load profile was also compared with typical demand profile

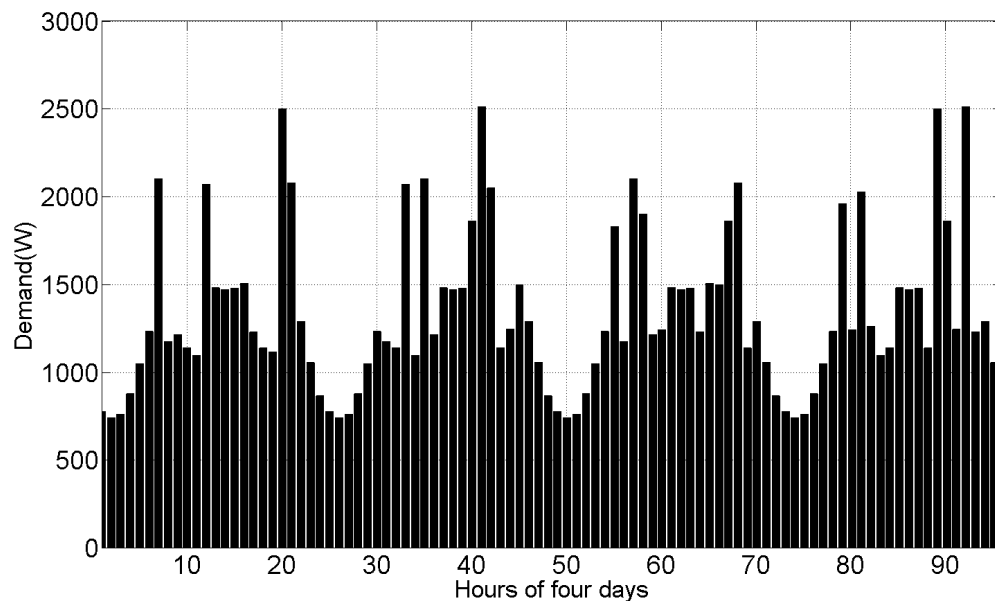


Fig. A.1 Hourly critical load of four days.

in regards to minimum, maximum, annual total load and the LPSP resulted due to this load profile with the system sized without considering the randomness in the annual hourly demand profile. The data is presented in the Table A.1. The peak and minimum hourly demand in each profile was found around 2509W and 742W respectively. The total amount of annual demand was almost similar. However, the size for each profile could not able to satisfy the other profile with desired reliability. This indicated that the temporal position of the peak demand profile effects the size of a HRES.

The optimized size of a HRES considering typical hourly electrical load of a day repeated throughout the year would not able to meet the desired reliability during the project life. The system which was optimized for zero LPSP, resulted in maximum LPSP of 0.100 percent with randomly varied demand profiles. This was equivalent to approximately 12kW loss of

power supply out of 12MW. This resulted in loss of power supply 9 (nine) hours out of 8760 hours a year. It was also evident from the different randomly varied annual demand profiles that total annual energy usage remained almost similar with the specified variation both in magnitude and temporal position. It was also found that the size of a HRES does not depend on the total amount of annual electrical, rather it depends on the hourly combination of energy usage. The LPSP as resulted with the system for the approximate critical combination of annual load reduced to 0.011 percent and the optimal size provide zero LPSP for any randomly varied demand profiles.

Table A.1 Comparison of annual total load and LPSP

Generated Load#	Total annual demand (W)	LPSP (%) with the system for		
		Typical Load	Critical load #1	Critical load #2
Load-A	12017289	0.023	0.000	0.000
Load-B	12001922	0.046	0.000	0.000
Load-C	11990207.78	0.057	0.000	0.000
Load-D	11990207.78	0.100	0.046	0.011
Load-E	12028337.29	0.068	0.000	0.011
Load-F	12003647.76	0.091	0.068	0.011
Load-G	12010086.7	0.057	0.000	0.011
Load-H	11980986.26	0.091	0.023	0.011
Load-I	12043927.33	0.091	0.046	0.011

Continued on next page

Table A.1 – Comparison of annual total load and LPSP(Continued)

Generated Load#	Total annual demand (W)	LPSP (%) with the system for		
		Typical Load	Critical load #1	Critical load #2
Load-J	12023739.7	0.100	0.000	0.011
Load-K	11978606.58	0.100	0.057	0.011
Load-L	11990694.28	0.068	0.000	0.011
Load-M	12018854.49	0.080	0.000	0.011
Load-N	12024047.86	0.068	0.011	0.00
Load-O	12024496.99	0.100	0.034	0.00
Load-P	12007032.11	0.110	0.091	0.000
Load-Q	12028337.29	0.100	0.046	0.011
Load-R	12003647.76	0.068	0.000	0.011
Load-S	11980986.26	0.057	0.000	0.011
Load-T	12043927.33	0.091	0.046	0.011
Load-U	12023739.7	0.100	0.000	0.011
Load-V	11978606.58	0.100	0.057	0.011
Load-W	11990694.28	0.068	0.000	0.011
Load-X	12018854.49	0.080	0.000	0.011